Geomech. Geophys. Geo-energ. Geo-resour. (2025) 11:38
https://doi.org/10.1007/s40948-025-00955-1

RESEARCH

Thermal damage in crystalline rocks: the role of heterogeneity

Yike Dang · Zheng Yang · Shangtong Yang · Xiaoyu Liu · Junlong Shang

Received: 16 December 2024 / Accepted: 11 March 2025

Abstract Accurately evaluating the impact of microstructural heterogeneity on thermal damage and failure mechanisms in crystalline rocks is crucial for geothermal energy development and the establishment of nuclear waste repositories. However, in thermal damage analyses of crystalline rocks using the discrete element method, most studies fail to account for the reduction in mineral mechanical and thermal properties caused by temperature increases. This study uses a Grain-Based model to simulate the microscopic mineral structure of crystalline rocks, focusing on analyzing the effect of heterogeneity. Thermal damage resulting from the uneven expansion of minerals is simulated by assigning specific thermal properties to each mineral. The temperature-induced degradation of mechanical and thermal properties is incorporated by introducing a temperature-dependent relationship for these characteristics in crystalline rocks. Along with moment tensor inversion theory, the microseismic behavior of crystalline rocks is explored to enhance understanding of rock failure mechanisms. The results indicate the following: (1) Thermal stress depends on the mineral's size, shape and arrangement. The sharp corners and edges of irregularly shaped minerals are more likely to become stress concentration points under the influence of temperature. (2) Peak strength gradually decreases with increasing heterogeneity and larger grain sizes. A negative correlation between quartz content and peak strength becomes more evident when the temperature

Y. Dang · Z. Yang
School of Human Settlements and Civil Engineering, Xi'an Jiaotong University, Xi'an 710049, China
e-mail: diryk0213@163.com

Z. Yang
e-mail: zyang@xjtu.edu.cn

Y. Dang · S. Yang
Department of Civil and Environmental Engineering, University of Strathclyde, Glasgow G1 1XJ, UK

S. Yang
Yunlong Lake Laboratory of Deep Underground Science and Engineering, Xuzhou 221100, China

S. Yang (✉)
State Key Laboratory of Intelligent Construction and Healthy Operation and Maintenance of Deep Underground Engineering, China University of Mining and Technology, Xuzhou 221100, China
e-mail: shangtong.yang@cumt.edu.cn

X. Liu
College of Sciences, Xi'an University of Science and Technology, Xi'an 710699, China
e-mail: xiaoyu-liu@xust.edu.cn

J. Shang
School of Engineering, The University of Manchester, Manchester M13 9PL, UK
e-mail: junlong.shang@manchester.ac.uk

Published online: 08 April 2025

exceeds 450 °C. (3) The combined effects of high temperature and heterogeneity lead to a more significant increase in the *b* value. Smaller grains increase the complexity of crack paths, leading to more frequent branching at grain boundaries and resulting in higher *b* values. (4) The uneven distribution of grain sizes is the primary factor influencing the mechanical properties of crystalline rocks, while grain size is a secondary factor. At the same temperature, samples with more uniform grain distributions and smaller grain sizes exhibit higher thermal stability.

Keywords Grain heterogeneity · Crystalline rocks · Thermal damage · Temperature dependence · Grain-Based model

1 Highlights

- A comprehensive evaluation of the effect of geometric and property heterogeneity on the thermal damage and failure mechanisms of crystalline rocks was conducted using the Grain-Based Model.
- By incorporating the temperature-dependent relationships of mineral mechanical and thermodynamic parameters, the numerical model effectively accounts for the effects of thermal expansion differences and the physicochemical changes of minerals on the thermal damage of crystalline rocks.
- The AE simulation based on moment tensor inversion revealed the impact of heterogeneity on the microseismic behavior of crystalline rocks.

2 Introduction

The heterogeneity of crystalline rocks is manifested in various aspects, such as mineral shape, grain size, and mechanical strength (Bass et al. 1995). Even samples of the same rock type can exhibit different mechanical behaviors due to this heterogeneity (Eberhardt et al. 1999a). The heterogeneity can cause stress concentration in localized areas within the sample, thereby influencing its overall mechanical properties (Blair and Cook 1998a). Minerals in crystalline rocks often exhibit irregular forms such as platy, blocky, or granular shapes, which are the primary sources of grain size heterogeneity, as shown in Fig. 1. The mineral's irregular shapes and distribution result from the rock's long-term formation process and geological structural activities. Accurately assessing the impact of heterogeneity on the thermal damage mechanisms and mechanical behavior of crystalline rocks at high temperatures is crucial for the successful development of geothermal energy (He et al. 2024) and the selection of sites for nuclear waste repositories (Dang et al. 2023b).

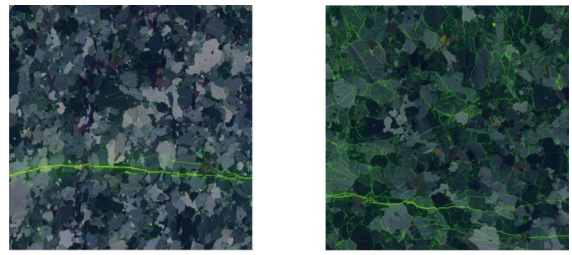

(a) Foliated granite (b) LdB granite

Fig. 1 Combined polarised and fluorescent microscopic image of granite (Åkesson 2008)

Crystalline rock heterogeneity can be categorized into two types: geometric heterogeneity and property heterogeneity. Geometric heterogeneity primarily involves factors such as variations in grain size and the uneven distribution of grain sizes (Liu et al. 2018; Wang et al. 2024b). Property heterogeneity, encompasses differences arising from the diversity of mineral components within the rock, including minerals strength disparities, differences in strength within and between grains, and the uneven distribution of thermodynamic parameters (such as specific heat, thermal expansion coefficient, and thermal conductivity). Researchers have conducted experimental and numerical simulation studies to investigate the effects of different heterogeneity factors in crystalline rocks.

Controlling grain size heterogeneity in laboratory experiments is challenging, so most research on its impact is conducted through numerical simulations. Figure 2a illustrates the relationship between grain heterogeneity index and peak strength at room temperature. Peng et al. (2017b) defined a heterogeneity index to reflect changes in grain size distribution and used particle flow modeling to examine how grain size heterogeneity influences rock strength and deformation behavior. Their findings indicate that as the heterogeneity index decreases, the peak strength

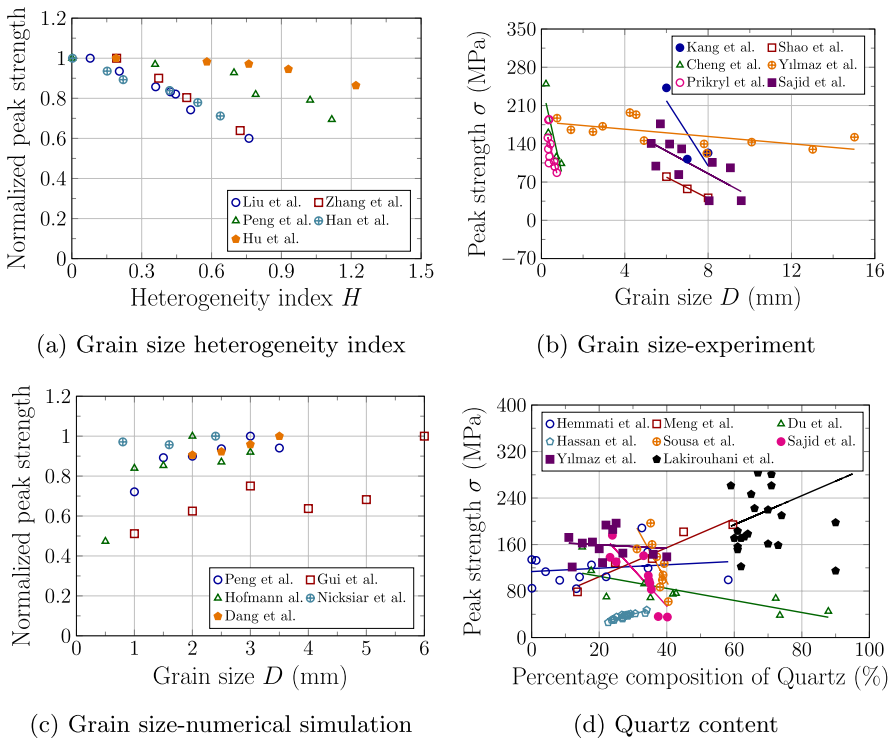

(a) Grain size heterogeneity index (b) Grain size-experiment

(c) Grain size-numerical simulation (d) Quartz content

Fig. 2 The relationship between grain size heterogeneity index, grain size, quartz content, and peak strength

of the rock increases, with grain size heterogeneity having little effect on the tensile strength. However, Liu et al. (2018) suggested that when there is significant variation in grain size within the rock, the calculation method proposed by Peng et al. (2017b) may no longer be applicable. They proposed an improved method for calculating the grain size heterogeneity index and investigated its impact on the mechanical properties of rocks. The sample's peak strength, crack initiation stress, and damage stress all decreased as the heterogeneity index increased. Yan et al. (2023) used the discrete element method (DEM) to explore heterogeneity's impact on shale's mechanical behavior. The results showed a negative correlation between the grain size heterogeneity index and the peak strength, with little effect on Poisson's ratio. Han et al. (2021) studied grain size heterogeneity's influence on rock's mechanical properties. They found that as the heterogeneity index increased, the rock's crack initiation stress, damage stress, and peak strength decreased linearly. Zhang et al. (2023) used the finite-discrete element method to simulate the failure characteristics of heterogeneous rock columns under different loading system stiffness. The results showed a negative correlation between grain size heterogeneity and peak strengths. Hu et al. (2023) studied the mechanical behavior of granite with varying grain heterogeneity index, finding that as the grain size heterogeneity index increased, the mechanical properties exhibited a declining trend.

There is some debate between experimental and numerical studies regarding grain size's impact on rocks' mechanical properties. Figure 2b shows the peak strength of samples with different grain sizes at room temperature. In Fig. 2b, the grain sizes presented by Kang et al. (2021) and Shao et al. (2014) are not quantitatively meaningful; they used a qualitative approach to distinguish grain sizes, categorizing them as fine, medium, and coarse. In the Fig. 2b, as the values on the x-axis increase, the grain size also increases. Kang et al. (2021) studied the physical and mechanical changes in three different granites with varying grain sizes. Their findings indicated that an uneven grain size distribution creates favorable paths for crack propagation and coalescence, with thermally induced microcracks appearing earlier with higher heterogeneity. Shao et al. (2014) found that granite with different grain sizes exhibited varying strength and elastic modulus changes at high temperatures. Notably, the development of thermal

cracks significantly influenced the failure behavior of the granite. Cheng et al. (2023) conducted uniaxial compression tests to examine the impact of grain size on the failure mechanisms of granite. The results showed that the strength and elastic modulus decreased as grain size increased, while plastic deformation characteristics became more pronounced. The finer-grained samples generated more dispersed and disordered microcracks, which helped to distribute stress and reduce local stress concentrations, resulting in higher strength and stiffness. Yılmaz et al. (2011) suggested that larger grain sizes create longer grain boundaries, which facilitate intergranular crack propagation, decreasing peak strength as grain size increases. Přikryl (2001) also identified a negative correlation between uniaxial compressive strength and the average grain size of rock-forming minerals. They suggested that this finding can be explained by Griffith's fracture theory, which posits that the stress required to cause brittle fracture is inversely proportional to the length of initial cracks in the material. If grain size represents the length of initial cracks, larger grain sizes would lead to lower peak strength in rock materials. Eberhardt et al. (1999b) argued that as grain size increases, longer grain boundaries and larger intergranular cracks provide extended weak paths for crack propagation, leading to decreased strength. Similarly, Sajid et al. (2016) showed that the peak strength gradually decreases as grain size increases. Although it is generally believed that fine-grained rocks have higher strength than coarse-grained rocks, the degree of recrystallization is also a crucial factor. It significantly affects the rock's water absorption capacity and porosity, which in turn negatively impacts its strength. However, Lakirouhani et al. (2020) conducted physical and mechanical tests on dolomite rocks with the same mineral composition but different grain sizes. The results showed a significant positive correlation between the rock's uniaxial compressive strength and grain size, the correlation coefficient reached 0.89. The phenomenon of peak strength increasing with grain size has also been observed in the experimental studies by Asemi et al. (2024). When studying the impact of grain size in laboratory experiments, most research uses average grain size or qualitative classification methods, which cannot avoid the influence of grain size heterogeneity.

Figure 2c shows the peak strength with different grain sizes obtained through numerical simulation. Peng et al. (2021) found that although the number of intergranular contacts in the model decreased as grain size increased, the proportion of intergranular cracks to total intergranular contacts gradually increased. This suggests that intergranular cracking intensifies with increasing grain size, and the numerical model's ability to sustain intergranular cracking is enhanced, leading to increased rock strength. In Peng et al.'s study, the shape of mineral grains was set as regular hexagons, thereby neglecting the effects of grain shape and grain size heterogeneity. Gui et al. (2016) suggested that the increase in peak strength with grain size is due to the reduction in grain interfaces. Hofmann et al. (2015) argued that the lower peak strength with smaller grain sizes is due to the higher degree of stress concentration in smaller grains. Nicksiar and Martin (2014) found that grain size does not affect peak strength when the mineral composition and grain size distribution remain constant. Overall, the bonding area between larger grains is relatively smaller, leading to fewer defects and microcracks during sample failure, which results in higher strength. In contrast, the bonding area between smaller grains is relatively larger, and there are more defects and microcracks within the crystals, reducing the strength of the rock. Dang et al. (2024a) also noted that the bonding area between large grains is relatively small, leading to fewer defects and microcracks during failure, thus contributing to higher overall rock strength. Conversely, smaller grains have a larger bonding area, with more defects and microcracks within the crystals, which reduces rock strength. Tian et al. (2020) suggested that, in granite, cracks are more likely to propagate between grains, and the macroscopic cracks in crystalline rocks usually exhibit a jagged pattern. As grain size increases, these macroscopic crack's jagged and interlocking effects become more pronounced, enhancing the peak strength. In the study of Tian et al. (2020), the grain size was qualitatively represented by the number of particles within a single cluster, using cluster units in PFC to simulate the grains. Peng et al. (2021) uniformly set the grain shapes as regular hexagons, a method that avoids the potential impact of grain size heterogeneity and grain shape on the experimental results. However, other researchers did not overlook the influence of grain size heterogeneity in their studies.

Different types of granite have varying mineral compositions (Cowie and Walton 2018), the hardness and thermodynamic properties of these minerals

also differ. It is well known that the thermal damage of rocks is caused by the anisotropic deformation of minerals when heated. When studying the thermal damage mechanisms of crystalline rocks, the effect of temperatures on the mechanical properties of the rock depends not only on the individual characteristics of the mineral grains but also on their interactions and collective response within the rock structure. Therefore, it is particularly important to investigate how different mineral compositions affect the mechanical properties, especially their thermodynamic properties. However, current studies on the impact of mineral composition on rock mechanical properties have mostly been conducted at room temperature. Figure 2d shows the relationship between quartz content and peak strength.

Hemmati et al. (2020) collected fifteen crystalline igneous rock samples from Iran and conducted uniaxial compression tests. The study highlighted that grain size has a more significant impact on rock strength than grain shape or mineral content. The size and content of potassium feldspar notably influence tensile strength. In contrast, compressive strength exhibits a more complex mechanism, seemingly controlled by the interfering effects of plagioclase and quartz structural properties. Meng and Pan (2007) explored the influence of petrological characteristics on the strength and failure of clastic rocks. They found that quartz content increases uniaxial compressive strength logarithmically, while the failure duration decreases logarithmically. Du et al. (2022) discovered that plagioclase content positively affects the strength of igneous rocks. In contrast, the strength of sedimentary rocks first increases and then decreases with the increase in plagioclase content. Additionally, increased quartz and potassium feldspar content significantly weakens rock strength. Hassan et al. (2019) found that increased quartz content significantly enhances rock strength. The positive impact of quartz on granite strength was more pronounced than the negative effects of feldspar and clay. Sousa (2013) explored the influence of mineral characteristics on its mechanical behavior. Their results indicated that as quartz content increases, peak strength gradually decreases. This decline in strength is attributed to the increased quartz-quartz contact and the reduced deformation capacity of the rock due to quartz's high hardness. Sajid et al. (2016) found a negative correlation between the content of quartz, plagioclase and the uniaxial compressive strength. The study emphasized that the average grain size of the rock is more important than the grain size of individual minerals in evaluating the rock's mechanical behavior. Yılmaz et al. (2011) examined the relationship between quantitative petrographic variables and mechanical properties in 12 types of granite. Their research revealed a significant negative correlation between potassium feldspar content and grain size with uniaxial compressive strength. While no significant correlation was found between quartz content and mechanical properties, there was a negative correlation between the average grain size of quartz and strength. Lakirouhani et al. (2022) investigated the effect of quartz content on the mechanical properties of rocks. The results showed that the peak strength of the samples increased with the quartz content. However, due to the presence of natural fractures in feldspar, an increase in feldspar content led to a decrease in the peak strength. The correlation between feldspar content and strength parameters was higher than that between quartz content and strength. Compared to grain size, analyzing mineral content is more challenging. It involves more uncontrollable factors, leading to the lack of a consistent conclusion regarding the influence of mineral content on rock strength.

When studying the impact of mineral composition on the mechanical properties of rocks, specimens are prepared by extracting rock blocks containing different mineral components from various locations. However, test data may be influenced by factors such as drilling depth, drilling techniques, and hydrogeological conditions, which can induce microcrack damage (Wong et al. 2018). Therefore, attributing differences in rock strength solely to mineral composition is not always reasonable. In addition to studying the effects of mineral composition on rock mechanical properties, research on grain size heterogeneity and grain size in the laboratory often faces the challenge of complex grain size characterization. Accurate measurement of grain size and distribution is crucial to studying the effects of failure mechanisms in crystalline rocks. Still, this process involves several complex steps. First, sample preparation is challenging, as it requires obtaining representative, undamaged thin sections from larger rock samples. This process can introduce artificial cracks or alter the original grain structure. Second, when observing and measuring grain size using a microscope, factors such as the

operator's skill and experience, the microscope's resolution, and the performance of image analysis software can all affect the results. Additionally, grains' three-dimensional distribution and orientation are difficult to fully capture in two-dimensional microscope images, which may lead to grain size and morphology misinterpretation.

Thermal damage in crystalline rocks can be categorized into two types: the first is damage caused by non-uniform deformation due to differential thermal expansion of minerals; the second is damage resulting from physicochemical processes such as mineral oxidation, dehydration, phase transitions, and melting. During the heating process, these physicochemical changes in minerals may lead to the deterioration of mineral structures, thereby altering the mechanical properties of the rock. However, many studies on thermal damage often overlook the impact of the mineral physicochemical reactions (Sun et al. 2021; Hu et al. 2023; Guo et al. 2023). In the studies by Dang et al. (2024a) and Tian et al. (2020), the grain size of quartz at 573°C was adjusted to indirectly reflect the impact of quartz phase transitions on thermal damage in rocks. However, other samples' minerals can also melt at high temperatures. For example, minerals such as potassium feldspar, sodium feldspar, and mica have melting points of around 600 °C (Shao et al. 2015). Chen et al. (2021) found that the calcite content decreased by 29.71% at 800 °C compared to room temperature but increased by 21.77% between 600 and 800 °C. This indicates that high temperatures can cause minerals to undergo physicochemical changes, affecting mechanical properties. Therefore, when conducting numerical simulations, the impact of mineral physicochemical changes on thermal damage should be considered.

This study employs the DEM to establish a Grain-Based Model (GBM) (Kong et al. 2021, 2024) to understand better the influence of heterogeneity in crystalline rocks on their thermodynamic behaviour and failure mechanisms. By simulating geometric heterogeneity through the GBM, the numerical model can more accurately represent the internal structure of real rocks, effectively simulating the microscopic mechanical behavior of rock materials, including crack development, deformability between minerals, and destructibility within minerals. Analyzing property heterogeneity is more complex and is usually not easily achieved through simple settings. Currently, the Weibull distribution is widely used to describe the non-uniform distribution of mechanical and thermodynamic parameters in rock samples, helping to more accurately predict and explain the mechanical behavior of rocks (Wang et al. 2024a). Some researchers have studied the effects of key parameters of the Weibull distribution on rock mechanical behavior (Zhao et al. 2022). In practice, it is challenging to quantitatively describe the heterogeneous distribution of natural rock strength, whether in actual engineering or laboratory-scale rock mechanics studies. Therefore, the Weibull distribution is introduced in this study to represent the heterogeneous distribution of mineral thermodynamic parameters and natural rock strength. The key parameters are selected based on recommendations from the literature without investigating the variations in these parameters.

Thermal damage in crystalline rocks can be divided into two components: (i) the uneven expansion of minerals upon heating, and (ii) the degradation of the mineral's mechanical and thermal properties due to the increase in temperature (Shi et al. 2023). In this study, uneven expansion is modeled by assigning specific thermal properties to each type of mineral. The temperature-induced degradation of mechanical and thermal properties is incorporated by introducing a temperature-dependent relationship for the mechanical and thermal characteristics of crystalline rocks. Additionally, based on moment tensor inversion theory, the method for simulating acoustic emission (AE) during rock failure at the microscale is established. The numerical simulation can capture the timing, location, and fracture intensity of AE events, allowing for microscopic analysis of how heterogeneity influences crystalline rocks' failure mechanisms and microseismic behavior.

3 Modeling procedure

3.1 Temperature dependence of thermal and mechanical properties of crystalline rocks

In discrete element simulations, thermal damage caused by thermal expansion differences is modeled by assigning corresponding thermodynamic parameters to minerals. The thermal expansion leads to bond breakage, thereby reflecting thermal damage induced by the uneven expansion of minerals. This study

introduces the damage coefficient that changes with temperature for the mechanical and thermodynamic parameters to simulate the thermal damage caused by mineral physicochemical reactions. The approach allows for a more comprehensive assessment of the thermal cracking behavior of rocks in high-temperature environments.

Wang and Konietzky (2019) proposed the temperature dependence relationships of the physical and mechanical parameters of granite under thermal effects, they summarized the fitting equations that describe the temperature dependence relationship. They applied the temperature dependence relationships to the simulation of granite's thermodynamic response in different numerical methods (Wang and Konietzky 2019; Wang et al. 2019, 2020, 2024a), yielding satisfactory simulation results. The normalized relationship between the thermal expansion coefficient and temperature, as proposed by Wang and Konietzky (2019), can be expressed as follows:

$$f_{\alpha/\alpha_0} = \begin{cases} (0.8383 - 0.00142T)^{(-1/1.7085)}, & 0 \le T \le 573 \\ (-5.416 + 0.0095T)^{(-1/1.5719)}, & 573 < T \le 625 \\ f_{T=625}, & 625 < T \le 800 \end{cases} \tag{1}$$

The normalized relationship between specific heat and temperature is:

$$f_{C_v/C_{v0}} = \begin{cases} 0.957 + 6.59 \times 10^{-4}T, & 0 \le T \le 573 \\ 1.173 + 1.238 \times 10^{-4}T, & 573 \le T \le 1000 \end{cases} \tag{2}$$

The normalized relationship between thermal conductivity and temperature is:

$$f_{k/k_0} = -5.8126 + 6.8485 \times 0.9995^T + 0.002172T, \quad 0 \le T \le 1200 \tag{3}$$

The curves of different parameters plotted according to equations 1-3, are shown in Fig. 3.

The following is the relationship between mechanical parameters and temperature. The relationship between normalized elastic modulus and temperature is:

$$f_{E/E_0} = \begin{cases} 1.2665/(1 + e^{-1.43+0.0034T}), & 0 \le T \le 600 \\ 1/(-109.953 + 17.542\ln(T)), & 600 < T \le 1250 \end{cases} \tag{4}$$

The relationship between normalized tensile strength and temperature is:

$$f_{\sigma/\sigma_0} = \begin{cases} 0.9912(1 - 4.1T/2483.30)^{(1/4.1)}, & 0 \le T \le 600 \\ 2.61e^{-0.0036T}, & 600 < T \le 1050 \end{cases} \tag{5}$$

The relationship between normalized cohesion and temperature is:

$$f_{c/c_0} = 0.1699(6.9845 - e^{0.001876T}), \quad 0 < T \le 1000 \tag{6}$$

The relationship between normalized internal friction angle and temperature is:

$$f_{\phi/\phi_0} = -6 \times 10^{-7}T^2 + 3 \times 10^{-5}T + 1.0034, \quad 0 < T \le 1000 \tag{7}$$

The relationship between normalized Poisson's ratio and temperature is:

$$f_{v/v_0} = \begin{cases} -7 \times 10^{-4}T + 1.0052, & 0 \le T \le 600 \\ 2.24/(1 + e^{13.11-0.02T}), & 600 < T \le 800 \end{cases} \tag{8}$$

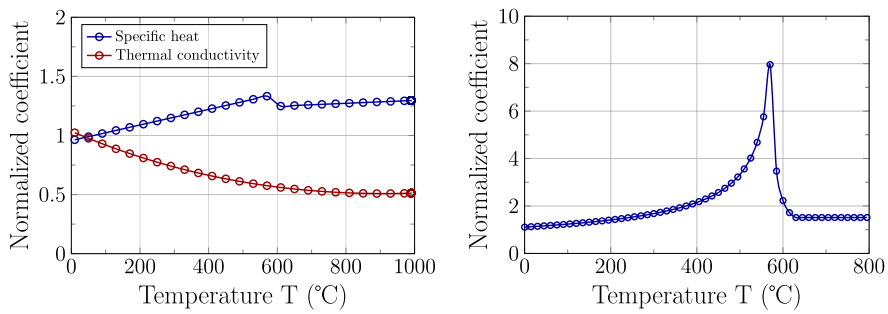

(a) Specific heat and thermal conductivity (b) Thermal expansion coefficient

Fig. 3 The variation curves of different thermodynamic coefficient with temperature

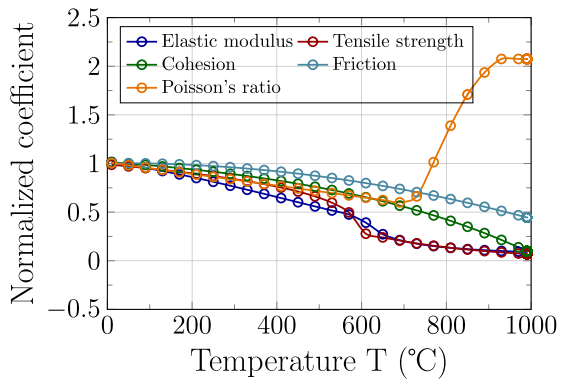

Fig. 4 The variation curves of different mechanical parameters with temperature

The temperature dependent curves of various mechanical parameters plotted according to equations 4–8 are shown in Fig. 4.

3.2 Modelling procedure and microparameters calibration

In this study, the numerical models for different heterogeneity factors in crystalline rocks were developed using the GBM. The PFC2D-GBM is constructed by overlaying a polygonal grain structure onto a bonded particle model, with interfaces represented by smooth joint contacts. The grain structure is filled with particles and described by a mesh of elements, edges, and nodes. Each grain is composed of a radially convex polygon made up of edges and nodes. Establishing the grain structure can refer to previous studies (Potyondy 2010).

This study's sample dimensions were 140 mm in height and 70 mm in width, after establishing the grain structure, it was filled with particles. The particle size is determined by repeated calibration, which requires that the particle size can better match the strength and failure mode of the sample in the experiment. The minimum particle size is 0.42mm, the maximum-to-minimum particle size ratio is 1.66 (Potyondy and Cundall 2004), the porosity of numerical model is 0.16. The particle size is uniformly distributed within this particle size range, and the numerical model has 10,464 particles. The generated grain structure is overlaid onto the particle model, and smaller particles are used to fill the grain structure, completing the construction of the GBM model. It should be noted that in all the models of the following studies, the particle size and porosity are kept consistent.

3.2.1 *Grain size heterogeneity*

Grain size heterogeneity in crystalline rocks refers to the uneven distribution of grain sizes. The grain size heterogeneity reflects the diversity in grain size and the irregularity of their distribution within the rock. Peng et al. (2017b) proposed a dimensionless coefficient, H, to calculate the heterogeneity of mineral grain size distribution in rocks. The heterogeneity index is mainly used to assess the variation in grain size; the larger the value of H, the greater the difference in grain sizes in the model, indicating a lower degree of uniformity. Liu et al. (2018) suggested that when the grain size of each mineral remains constant or varies within a small range, the method proposed by Peng et al. (2017b) for calculating the grain heterogeneity index is suitable. In fact, the distribution of mineral grain sizes in rocks is heterogeneous. When the range of grain size variation is large, the error of the method proposed by Peng et al. (2017b) will increase. Based on this, Liu et al. (2018) proposed a new formula for calculating the average grain size, which better reflects the average grain size in rocks, as follows (Liu et al. 2018):

$$d_{\text{new}} = \frac{1}{\sqrt{\sum_{i=1}^{m} \frac{w_i}{\overline{d_i}^2}}} \tag{9}$$

Where w_i and $\overline{d_i}$ are the volume fraction and mean grain size of minerals, and m is the number of minerals.

Considering the variation in grain size within each mineral, Liu et al. (2018) used the minimum, average, and maximum grain sizes of each mineral to assess the variation in grain sizes within the rock. The new heterogeneity coefficient is defined as follows (Liu et al. 2018):

$$H_{\text{new}} = \frac{1}{3m} \sum_{i=1}^{m} \sum_{j=1}^{3} \left| \frac{d_{ij}}{d_{\text{new}}} - 1 \right| \tag{10}$$

In the equation, d_{i1}, d_{i2}, d_{i3} represent the minimum, average, and maximum grain sizes of mineral i. This study will reference the method proposed by Liu et al.

(2018) to define models with different grain heterogeneity coefficients.

Figure 5 shows the numerical models constructed with different grain heterogeneity coefficients, with the heterogeneity coefficient H ranging from 0 to 0.92. The numerical samples consist of Plagioclase (45%), K-feldspar (10.7%), Quartz (6.8%), and Biotite (37.5%), as shown in Table 1. The proportions of these mineral components remain constant across numerical models with different heterogeneity coefficients.

According to Kelly et al. (1994) study on the grain size of LdB granite, Plagioclase has the largest average grain size, followed by K-feldspar, with Quartz and Biotite having the smallest average grain sizes. Based on the research findings (Peng et al. 2017b; Hu et al. 2023), our study follows the grain size distribution pattern: Plagioclase > K-feldspar > Quartz > Biotite. In the numerical model, each mineral's composition and number of particles remain consistent.

We generated models with different grain size heterogeneity coefficients by controlling the grain sizes distribution and using the heterogeneity coefficient calculation method proposed by Liu et al. (2018). The larger heterogeneity coefficient indicates a broader grain size distribution and higher heterogeneity. The distribution of grain sizes with varying coefficients of heterogeneity is shown in Table 2. Han et al. (2021) pointed out that due to the different impacts of grain size and grain size heterogeneity, there is no clear relationship between the average grain size and the grain size heterogeneity index in Table 2.

It is important to note that the grain sizes are distributed in a regular hexagonal pattern in the numerical model with a heterogeneity coefficient $H = 0$. Although the hexagonal grain structure differs from typical rock samples, this approach effectively eliminates the influence of factors other than mineral composition on mechanical behavior and failure. Thus, any changes in the mechanical properties of the numerical model can be entirely attributed to changes in mineral composition. This allows for a clearer understanding of the impact of grain heterogeneity on the mechanical behavior and failure of crystalline rocks by comparing this model with others (Wong et al. 2018). For the numerical model with a heterogeneity coefficient $H = 0.17$, only the ratio between the smallest and largest grain sizes was controlled without specifically setting the grain sizes for the four minerals. This configuration produces a numerical model with a uniformly distributed grain size, enabling comparative analysis with other numerical models to explore the effects of grain size distribution uniformity on mechanical behavior.

Table 1 The mineral composition of sample

Mineral	Percentage /%
Plagioclase	45
K-feldspar	10.7
Quartz	6.8
Biotite	37.5

The cumulative grain size distribution curves with different grain size heterogeneity are shown in Fig. 6. The steeper the curve, the smaller the variability in grain size, indicating a lower grain size heterogeneity index. Conversely, when the grain size distribution range is wider, meaning the ratio between the largest and smallest grain sizes is larger, the heterogeneity index increases. Additionally, samples with a high grain size heterogeneity coefficient typically exhibit a stepped characteristic in the cumulative passing curve, indicating a noticeable discontinuous gradient in grain size distribution. This discontinuity in size distribution and the broad range of grain sizes leads to higher heterogeneity. Figure 7 shows the distribution of intergranular and intragranular contacts with different heterogeneity index, revealing no relationship between the number of intergranular and intragranular contacts and the heterogeneity coefficient in the numerical models.

3.2.2 Grain size

The heterogeneity of grain size distribution and particle shape significantly impacts the mechanical behavior of samples. In exploring the influence of grain size on mechanical behavior, we adopted the method used by Peng et al. (2021) and chose to use a hexagonal grain distribution. As shown in Fig. 5, using hexagonal grain shapes helps eliminate the potential influence of grain size distribution heterogeneity and grain shape on the experimental results. Figure 8 presents the numerical models with different grain sizes.

Hofmann et al. (2015) attributed the peak strength increased with larger grain sizes to the higher stress concentration in smaller grain sizes, which reduced

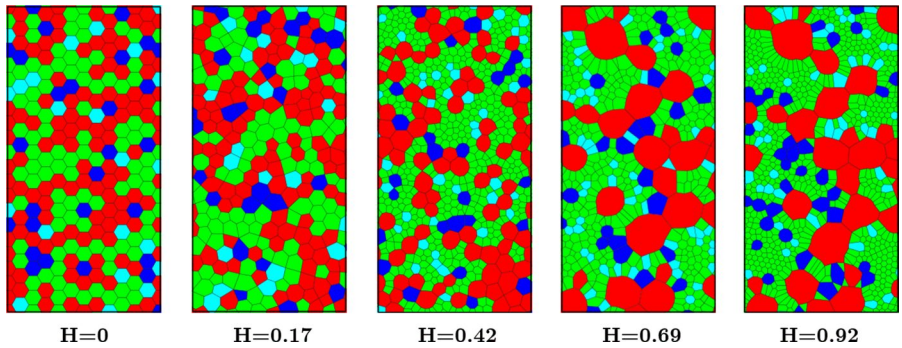

Fig. 5 Numerical models with different grain size heterogeneity coefficients. The red, blue, green, and cyan geometries represent Plagioclase, K-feldspar, Biotite, and Quartz, respectively

the peak strength due to the smaller number of particles within each grain. Peng et al. (2021) designed two experimental scenarios to test this conclusion thoroughly. In the first scenario, the number of particles within each grain increased as the grain size increased. In the second scenario, although the grain size increased, the number of particles within each grain remained approximately constant, they observed that even when the number of particles was roughly the same, the strength generally increased with larger grain sizes. This indicates that the rock strength was not directly related to the number of particles within the grains. Instead, the grain size had a more direct and significant impact on the rock strength. This finding suggests that stress concentration caused by particle distribution is not the primary determinant of rock strength; rather, the grain size plays a more crucial role. Therefore, when studying the effects of grain size heterogeneity, grain size, and subsequent mineral composition on the mechanical behavior of crystalline rocks, the size of the particles in each model is kept consistent.

Table 2 Grain size statistics in numerical models with different grain size heterogeneity

H	Average grain size D (mm)	Type	D_{min} (mm)	D_a (mm)	D_{max} (mm)
0.17	3.29	P	2.5	3.38	4.15
		B	2.5	3.38	4.15
		K	2.5	3.38	4.15
		Q	2.5	3.38	4.15
0.42	2.1	P	3	4.06	4.98
		B	1.2	1.62	1.99
		K	2.5	3.38	4.15
		Q	1.7	2.31	2.82
0.69	2.23	P	3	7.38	12
		B	1.2	1.82	1.44
		K	2.5	3.42	3.25
		Q	1.7	2	2.21
0.92	1.67	P	3	7.34	12
		B	1.2	1.35	1.44
		K	2.5	3.24	3.88
		Q	1.7	2.09	2.38

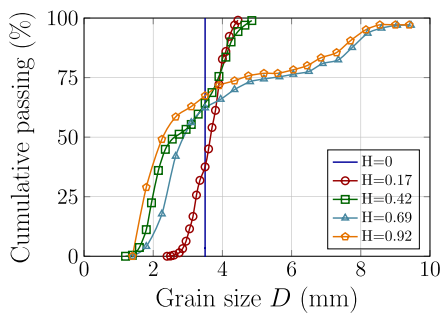

Fig. 6 Grain size distribution curves with different heterogeneity index

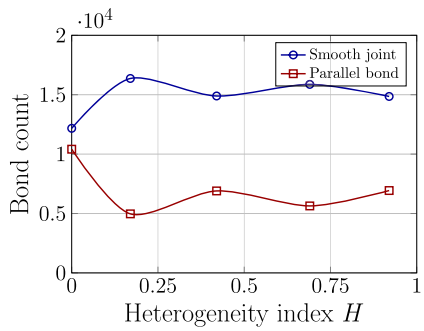

Fig. 7 The intergranular and intragranular contact numbers with different heterogeneity index

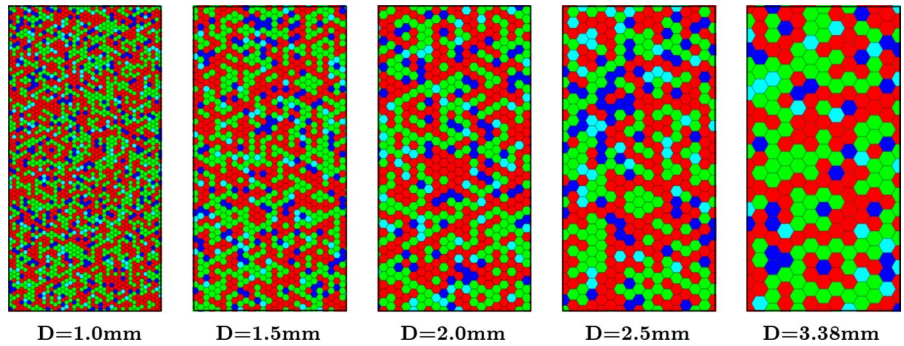

Fig. 8 Numerical models with different grain sizes

3.2.3 Mineral composition

To study the impact of mineral composition on the thermodynamic behavior of crystalline rocks, we constructed numerical models with different mineral compositions, as shown in Fig. 9. The construction process was based on the study by Wong et al. (2018). The Biotite content in each numerical model is kept constant at 10%. The contents of Quartz, Plagioclase, and K-feldspar vary between 10 and 70%. To eliminate the influence of grain size heterogeneity and differences in grain size on the results, the grain size, grain shape, and the number and size of particles in each numerical model are kept consistent. The rock type may change depending on the variation in mineral composition. According to the Quartz-Alkali Feldspar-Plagioclase classification system (Wong et al. 2018), the corresponding rock types for each numerical model are shown in Table 3.

3.2.4 Numerical model parameter setting and thermal treatment process

After establishing the numerical model, a trial-and-error method is adopted for parameter calibration (Dang et al. 2024b). The laboratory tests were conducted on thermal treated samples. Therefore, during parameter calibration, the numerical model must undergo the same thermal treatment as the experiment, followed by uniaxial compression testing. Finally, the mechanical parameters from the laboratory tests are compared with the simulation to verify the parameters, ensuring the accuracy of the numerical model.

The thermal treatment process is as follows: (1) Specify the thermal parameters of each mineral at room temperature. The model is iteratively updated until the imbalance force ratio is less than or equal to 1.0e−4 (The unbalanced force ratio is defined as the ratio between the maximum unbalanced force and the average force of all particles), indicating that the model has reached a stable state. (2)

Table 3 Mineral composition and corresponding rock types in numerical model

Model	Rock type	Biotite	K-feldspar	Plagioclase	Quartz
M1	Quartz-rich granitoid	10	10	10	70
M2	Quartz monzodiorite	10	10	70	10
M3	Quartz syenite	10	70	10	10
M4	Quartz monzonite	10	30	40	20
M5	Syeno-granite	10	30	30	30
M6	Monzo-granite	10	10	40	40
M7	Syeno-granite	10	30	10	50
M8	Syeno-granite	10	10	20	60
M9	Quartz monzonite	10	30	50	10
M10	Quartz monzonite	10	10	60	20
M11	Quartz syenite	10	50	20	20

During thermodynamic calculations, both thermal and mechanical computation switches are turned on, and the model is heated to the target temperature T at a rate of 25 °C /step (To avoid thermal shock. The target temperatures are set at 150 °C, 300 °C, 450°C, 600°C, 750°C, and 900°C, respectively.). After reaching the target temperature, the thermodynamic computation switch is turned off, and the model is run for 100 timesteps to simulate the uniform heating process. After each heating stage, the model is iterated to a balanced state (the criteria for model equilibrium are as specified in step (1)). (3) Return to step (1). Follow the steps outlined above to subject the samples to heat treatment until the target temperature is reached. Once the heating calculation is complete, the model's target temperature is set to -T, and the above steps are repeated to simulate the cooling process.

After the thermal treatment is completed, an axial load is applied. The loading is displacement-controlled, to ensure the model remains in a quasi-static state during loading, the sample is loaded at a rate of 0.02 m/s until failure, with the loading rate based on the study by Zhang and Wong (2014). The friction coefficient between the sample and the loading plate is 0. Specifying the thermodynamic parameters of each mineral, such as thermal conductivity, coefficient of thermal expansion, and specific heat, is crucial for accurately reflecting the impact of temperature on the mechanical properties of rocks (Tang et al. 2023a, b). However, many researchers fail to accurately assign the thermodynamic coefficients of individual minerals in numerical simulations (Zhao et al. 2020), which can lead to inaccurate results. To more effectively study the effects of high temperature on the thermodynamic properties of rocks, we have explicitly assigned the thermodynamic coefficients for each mineral in our simulations, as shown in Table 4.

Table 4 Thermal parameters of minerals (Guo et al. 2023; Wu et al. 2020; Wang et al. 2024a)

Minerals	Thermal expansion coefficient, 10^{-6}/°C	Specific heat, J/kg·°C	Thermal conductivity, W/m·°C
Plagioclase	14.1	1081	2.4
Biotite	3.0	773	2.3
Quartz	24.3	700	7.69
K-feldspar	8.7	1081	2.3

Shi et al. (2019) used the PFC to explore the impact of scale and shape parameters within the Weibull distribution on rock's mechanical performance and deformation failure. Their findings suggest that the scale parameter α of 1.0 and the shape parameter β of 3.8 provide a more accurate simulation of the deformation process. In this study, the bond strength between particles in the sample adhered to a Weibull distribution, with the scale and shape parameters fixed at 1 and 3.8, respectively. The thermodynamic parameters of each mineral, such as specific heat, thermal expansion coefficient, and thermal conductivity, also follow a Weibull distribution. The scale and shape parameters of the Weibull distribution are set according to the study by Wang et al. (2019). Table 5 summarizes the settings for the scale and shape parameters of the Weibull distribution in the numerical model.

To achieve the temperature dependence of mechanical properties, the stiffness and strength parameters of contacts and bonds are adjusted to vary with temperature (Shi et al. 2023). For the thermodynamic parameters, the thermal properties of minerals are dynamically modified according to temperature changes to achieve temperature dependence. As discussed earlier, the strength parameters of minerals are derived based on their hardness values. When setting parameters, we referred to previous studies (Peng et al. 2017a, b) for the hardness values of each mineral, and the strength values of the minerals follow the order: Quartz > Plagioclase > K-feldspar > Biotite. The determined microparameters are listed in Table 6.

It should be noted that in our previous research (Yang et al. 2024; Dang et al. 2024c), we investigated the combined effects of pre-existing fractures and

Table 5 Weibull distribution coefficients for thermal and mechanical properties of minerals (Shi et al. 2019; Wang et al. 2019)

Type	Parameters	α	β
Mechanical	Elastic modulus, E	1	3.8
	Cohesion, c	1	3.8
	Tensile strength, σ	1	3.8
Thermal	Thermal expansion coefficient, α_t	1.101	4.1
	Specific heat, C_v	1.038	14
	Thermal conductivity, k	1.115	1.6

Table 6 Micromechanical parameters of different types of minerals

	Microparameters	Value			
		Plagioclase	Biotite	Quartz	K-feldspar
Minerals	Effective modulus of particle, E_c (GPa)	13	8	18	11
	Stiffness ratio of particle, k_n/k_s	1.7	1.1	1	1.6
	Effective modulus of bond, E_b (GPa)	13	8	18	11
	Stiffness ratio of bond, k_{nb}/k_{sb}	1.7	1.1	1	1.6
	Friction coefficient, f	1.2	1.2	1.2	1.2
	Particle density, ρ (kg/m^3)	2650	3000	2640	2650
	Tensile strength, σ_c (MPa)	93	88	98	93
	Cohesion, c (MPa)	266	250	281	266
	Friction angle, ϕ (°)	30	30	30	30
Interface	SJ shear normal stiffness factor, α_{sf}	0.8			
	SJ contact normal stiffness factor, α_{nf}	0.6			
	SJ bond tensile strength, σ_s (MPa)	36			
	SJ bond cohesion, c_s (MPa)	133			
	SJ bond friction angle, ϕ_s (°)	30			
	SJ bond friction coefficient, f_s	1.2			

temperature on the failure modes of crystalline rocks. Additionally, using discrete element numerical simulations, we analyzed the impact of pre-existing fractures and temperature on crack propagation in crystalline rocks from a micro-mechanical perspective. The dimensions of the numerical model are 140 mm in length and 70 mm in width, with the pre-existing fracture measuring 20 mm in length, 1.5 mm in width, and a 45° inclination, consistent with the laboratory samples.

According to the statistical data (Martin 1993), the grain size of LdB granite ranges from 3 to 9 mm. To reflect the grain heterogeneity of crystalline rocks while also considering computational efficiency, we generated a numerical model that incorporates grain heterogeneity for parameter calibration. That is, the model with $H = 0.42$ shown in Fig. 5, the average grain size of the model is 2.1 mm. Unlike Fig. 5, the numerical model used for calibrating the micromechanical parameters includes a pre-existing fracture with a length of 20 mm, a width of 1.5 mm, and an inclination angle of 45° (The pre-existing fracture is created by removing the particles in the central region of the model.). The purpose is to compare it with the experimental results of specimens with a pre-existing fracture at a 45° angle from the laboratory tests. Based on this model, we calibrated the micromechanical parameters for different types of minerals and applied them to the study of the micro-failure mechanisms in crystalline rocks with pre-existing fractures, as well as in the present study.

The comparison of stress–strain curves, elastic modulus, and peak strength of samples after different temperature treatments with experimental results is shown in Fig. 10. As seen in Fig. 10, except for the sample with a thermal treatment temperature of 150°C, the mechanical parameters obtained from the simulations align well with the experimental results, validating the accuracy of the microparameters. However, when using the DEM to study the thermal damage of rocks, some researchers have found that their simulations yield mechanical parameters that differ significantly from experimental results due to the limited factors considered (Wu et al. 2020; Tian et al. 2020; Guo et al. 2023), with the discrepancies being particularly pronounced at higher temperatures.

The uniaxial compression tests were conducted on samples after thermal treatments to demonstrate the necessity of considering mineral physicochemical changes in studying rock thermal damage, as shown in Fig. 10. However, due to the extensive range of factors analyzed in this study, the rock's mechanical properties and failure mechanisms were only examined for data ranging from room temperature to thermal treatment temperature of 600°C. To comprehensively analyze the thermal damage mechanisms of crystalline rocks across different temperature ranges,

the maximum temperature for thermal damage analysis remains set at 900°C.

4 The effect of heterogeneity on the mechanical properties of crystalline rocks

4.1 The effect of grain size heterogeneity on the mechanical properties

Figure 11 shows the peak strength and elastic modulus with different heterogeneity index after thermal treatments. The peak strength and elastic modulus decrease as the temperature increases for the models with different heterogeneity index. Particularly when the temperature exceeds 450°C, there is a significant reduction in the peak strength. This indicates that the thermal damage degree increases with the temperature, leading to a substantial decline in their mechanical properties. For samples with a heterogeneity index of 0, where all grain sizes are uniform, the external stress is more evenly distributed within the sample, thereby avoiding stress concentrations arising from grain size differences. Since stress concentration is significantly reduced in samples with a heterogeneity index of 0, their peak strength remains consistently higher. In the model with a heterogeneity index of 0.42, the smaller average grain size results in lower peak strength than 0.92 within the temperature range of 25°C~450°C. This indicates that grain size significantly impacts the mechanical properties of crystalline rocks.

Figure 11b shows that the heterogeneity index has little effect on the elastic modulus. The elastic modulus reflects the stress–strain relationship during small deformations, where the grain microstructure and intrinsic elastic properties dominate. Although grain size heterogeneity exists, the elastic modulus of individual grains remains largely unchanged, keeping the average modulus of the sample stable. In the elastic stage, stress distribution is relatively uniform, and even with varying heterogeneity indices, the minimal deformation ensures uniform stress transfer between grains, preventing significant stress concentrations. As a result, the elastic modulus remains largely unaffected by the heterogeneity index.

Figure 12a presents the peak strength and elastic modulus with varying heterogeneity index. The peak strength generally decreases as the heterogeneity index increases. The grain size heterogeneity causes uneven stress distribution within the rock, the stress concentration zones are more likely to form at the boundaries between large and small grains, making these areas more susceptible to cracking and failure, thus reducing the rock's overall strength. In samples with higher heterogeneity index, the interfaces between large and small grains may serve as weak points, promoting crack propagation along these boundaries. The complexity of the crack propagation paths further affects the failure behavior and strength. Consequently, samples with greater heterogeneity typically exhibit lower strength due to increased stress concentration and crack propagation.

Blair and Cook (1998a, 1998b) pointed out that local stress disturbances caused by grain shape irregularities have a significant impact on the macroscopic properties of rocks. Lan et al. (2010) studied the effect of grain heterogeneity on the mechanical behavior of brittle rocks. The results showed that samples with a more uniform grain size distribution exhibited more uniform stress distribution when subjected to external loads. When the rock is subjected to compressive stress, the local tensile stress heterogeneity induced by grain heterogeneity promotes the initiation, propagation, and interaction of tensile cracks. Moreover, samples with stronger grain heterogeneity exhibited a more uniform internal stress distribution, resulting in higher compressive strength. Dang et al. (2024a) also showed that thermal cracks tend to occur along the short axis of mineral grains and at anomalous interfaces, primarily due to the stronger stress singularities in these regions. These studies further illustrate that the non-uniformity of grain size leads to uneven internal stress distribution in rocks, with stress concentration areas forming more easily at the boundaries of large and small grains. As a result, these regions are more likely to crack and fail, thereby reducing the overall strength of the rock.

Figure 12b illustrates the relationship between elastic modulus and heterogeneity index. Between 25~450°C, the elastic modulus shows little variation across different heterogeneity index. However, at 600°C, the elastic modulus slightly decreases as the heterogeneity index increases, though this reduction is relatively modest.

Figure 13 summarizes the relationship between heterogeneity index and normalized peak strength

from various studies. The relationship between grain heterogeneity and peak strength found in this study aligns with those reported by other researchers, showing a general trend of decreasing peak strength as the heterogeneity index increases. Notably, in some temperature conditions, the peak strength with a heterogeneity index of 0.42 is even lower than that of samples with a heterogeneity index of 0.92. Figure 5 shows that in the model with a heterogeneity index of 0.42, a large number of small-sized grains are distributed in the main load-bearing area of the sample, which increases the number of grain boundaries in this region. Table 2 also indicates that, except for the sample with a heterogeneity index of 0.92, the sample with a heterogeneity index of 0.42 has the smallest average grain size. Since grain boundaries are the weakest areas in terms of mechanical properties within a material, their presence under external load reduces the local compressive strength, leading to a lower overall strength of the material. In contrast, in the model with a heterogeneity index of 0.92, the main load-bearing area of the sample is dominated by larger grains. Larger grains typically have higher compressive strength, allowing these regions to effectively resist external loads and exhibit stronger overall strength. Furthermore, the presence of larger grains reduces the number of grain boundaries, decreasing the likelihood of local plastic deformation and enhancing the material's compressive performance.

Therefore, although the model with a heterogeneity index of 0.42 is theoretically expected to have higher strength, the high density of small grains in the main load-bearing area and the increased number of grain boundaries lead to local weakening of the material during compression, which reduces its strength. In contrast, the model with a heterogeneity index of 0.92, having more large grains in the main load-bearing area and fewer grain boundaries, enhances the material's compressive performance, resulting in higher strength. This difference highlights the significant impact of grain size, grain boundary distribution, and the distribution characteristics of minerals in the main load-bearing area on compressive strength. The variation in the heterogeneity index directly affects the combination and distribution of these factors, leading to different strength performances.

4.2 The effect of grain size on the mechanical properties

Figure 14 shows the peak strength and elastic modulus with different grain sizes after thermal treatment. Both properties decrease as the temperature increases, consistent with previous analysis. High temperatures induce thermal stress within the granite, causing microcrack formation due to the differing thermal expansion coefficients of its mineral components. As temperature rises, thermal damage intensifies, significantly reducing the material's mechanical properties. Additionally, high temperatures weaken the bonding between mineral particles, loosening the structure and making the rock more prone to deformation, which is reflected in the decreasing elastic modulus.

Figure 15 shows the relationship between peak strength, elastic modulus, and grain size for different samples. Figure 15a shows that without considering grain size distribution heterogeneity, peak strength increases with larger grain sizes. This is because larger grain boundaries resist crack propagation, requiring more energy for failure and thus increasing peak strength. In contrast, smaller grain sizes allow cracks to traverse more easily, reducing peak strength. Larger grains enhance both crack resistance and overall structural integrity, leading to higher strength under external forces.

Additionally, grain boundarie's strength largely determines the rock's overall strength. Samples with larger grains have fewer grain boundary contacts, leading to a smaller weakening effect at the boundaries. Conversely, samples with smaller grains have more grain boundaries, with a more pronounced weakening effect, contributing to the lower peak strength observed in smaller grain size samples.

Figure 15a shows the relationship between grain size and elastic modulus. Under heat treatment conditions ranging from room temperature to 300°C, the impact of temperature on the structure and physical properties is minimal, resulting in little difference in elastic modulus across samples with different grain sizes. However, when the temperature exceeds 300°C, the thermal stress caused by the differences in thermal expansion coefficients between different minerals becomes more pronounced, particularly at grain boundaries. In samples with larger grains, although there are fewer grain boundaries, the stress

concentration within each grain is more significant, forming more microcracks. These microcracks reduce the rock's overall stiffness, lowering the elastic modulus. Additionally, at higher temperatures, the larger volume of the grains results in uneven thermal expansion within the grains, causing stress concentration and microcrack propagation. These internal stress concentration areas significantly reduce the stiffness of the grains and the overall elastic modulus.

Figure 16 compares the results of this study with those of other researchers regarding the effect of grain size on the peak strength of crystalline rocks. The findings of this study align with the general trend observed in the literature: peak strength tends to increase with larger grain size. It is important to note that, apart from the studies by Peng et al. (2021) and this study, other researchers did not disregard the effects of grain shape and heterogeneity. The relationship between grain size and peak strength in Fig. 16 does not align with the experimental conclusions. However, similar trends of increasing peak strength with larger grain size have been observed in the experimental studies by Lakirouhani et al. (2020) and Asemi et al. (2024).

Experimental studies often involve complex factors, such as natural defects in the rock, the presence of microcracks, and porosity, which numerical simulations cannot fully account for. Grain boundaries, considered weak points in the rock structure, are critical factors influencing the strength of crystalline rocks (Peng et al. 2021; Kong et al. 2024). However, these factors are challenging to characterize through experimental means, making it difficult for numerical simulations to accurately incorporate experimental findings when setting mechanical parameters at grain boundaries. In numerical simulation studies, microcracks at grain boundaries are typically disregarded, and the strength at these boundaries is assumed to be uniform (Aboayanah et al. 2024; Hamediazad and Bahrani 2024), with the mineral's strength determined by its hardness (Shang 2020). Researchers often compare experimental and numerical simulation results to determine the strength parameters for grains and grain boundaries. However, whether the assumed bonding strength at grain boundaries in simulations accurately reflects the behavior of real rock samples remains debatable. This discrepancy may be the primary reason for the inconsistent conclusions between numerical simulations and experimental studies regarding the effect of grain size on rock strength.

In laboratory studies on the influence of grain size on the mechanical behavior of crystalline rocks, the average grain size is typically used (Kang et al. 2021; Yılmaz et al. 2011; Shao et al. 2014). In other words, these studies mainly focus on the effect of average grain size on mechanical behavior, while factors such as the heterogeneity of grains-including mineral composition, grain shape, and grain arrangement-are not considered. However, the mechanical behavior of crystalline rocks is primarily influenced by their grain heterogeneity structure.

4.3 The effect of quartz content on the mechanical properties

We generated numerical models with varying mineral compositions to investigate the impact of mineral composition on the thermodynamic behavior of crystalline rocks. Table 3 shows that the proportions of three minerals (excluding biotite) were controlled. Therefore, under certain mineral compositions, the mechanical parameter values may vary. For example, when the quartz content is 10%, the peak strength for quartz may include three different values. Figure 17 shows the relationship between quartz compositions and peak strength after thermal treatment. The red lines represent the fitted relationship between composition and peak strength, with k as the slope.

A negative correlation exists between quartz content and peak strength at all temperatures, though it is less pronounced from room temperature to 300°C. However, above 300°C, peak strength gradually decreases as quartz content increases. This because quartz has a significantly different thermal expansion coefficient compared to other minerals, leading to the generation of thermal stress between minerals during thermal treatment. The stress promotes the formation and propagation of internal microcracks. The higher the quartz content, the more thermally induced cracks form, weakening the overall strength of the rock. The high thermal expansion coefficient of quartz causes its thermal expansion behavior at high temperatures to differ from surrounding minerals, leading to stress concentration and stress redistribution within the sample. This effect becomes more pronounced at high temperatures. Graphs for 450°C and 600°C show that high temperatures amplify quartz's negative

effects, such as microcrack formation, weakened grain boundaries, and stress concentration. Another factor is quartz's high brittleness, which prevents it from effectively mitigating stress concentration when subjected to external forces. This causes stress to concentrate around quartz particles, leading to localized failure. As the quartz content increases, the stress concentration effect becomes more pronounced, reducing the peak strength. These factors combined make the negative influence of increased quartz content on rock strength more significant under high-temperature conditions.

Figure 18 shows the relationship between the quartz composition and elastic modulus after thermal treatment. The correlation between quartz composition and elastic modulus is higher for any temperature condition than that between quartz composition and peak strength. As the temperature increases from room temperature to 450°C, the slope of the curve gradually decreases.

From room temperature to 300°C, temperature has minimal effect on mineral structure and grain boundary properties. Within this range, quartz retains its mechanical properties, resisting phase changes and structural alterations, positively influencing the elastic modulus. As the temperature nears 450°C, thermal stress-induced microcracks increase, weakening quartz's positive effect. At 600°C, microcracks and porosity increase significantly, and quartz's high thermal expansion promotes crack propagation, further weakening the structure. This results in a decrease in elastic modulus as quartz content increases.

Quartz has one of the highest stiffness and elastic modulus among common minerals. As quartz content increases, the sample's stiffness and elastic modulus improve due to quartz's resistance to deformation. The rock's ability to resist deformation depends on the weighted average of its minerals' resistance based on their volume fractions. Increasing quartz content effectively raises the proportion of minerals with a high elastic modulus, enhancing the sample's elastic modulus. However, despite the increase in elastic modulus with higher quartz content, the slope of this positive correlation gradually decreases with rising temperature due to stress and microcrack effects caused by thermal expansion. Additionally, quartz undergoes an α-β phase transition at 573°C, accompanied by volume changes and structural reorganization, generating additional stress and microcracks within the grains and at grain boundaries. While quartz enhances elastic modulus at lower temperatures, this effect diminishes or becomes negative at higher temperatures, especially near the phase transition temperature.

As shown in Table 3, the proportions of the other three minerals vary when one mineral content is the highest in most models. This imbalance complicates understanding the effect of mineral content on thermodynamic behavior under high temperatures. To address this, based on the models in Table 3, we controlled the content of plagioclase, potassium feldspar, biotite, and quartz, increasing each from 25 to 85% in increments of 15%. If the mineral with the highest content is referred to as the main mineral, the proportions of the other three minerals remain consistent. While this approach may not perfectly mirror natural compositions, it isolates the effect of mineral composition, providing a clearer understanding of its impact on thermal damage and mechanical properties at high temperatures. Figure 19 compares the results of this study with those from the literature. In this study, when the effects of grain size heterogeneity, grain shape, and other mineral compositions were ignored, the peak strength of the samples showed a slight decreasing trend with increasing quartz content.

The general understanding regarding the relationship between quartz content and peak strength in crystalline rocks is that peak strength increases with higher quartz content. However, some experiments have observed a negative correlation between quartz content and peak strength, as shown in Fig. 2d. Cowie and Walton (2018) compiled the mechanical properties of 58 different types of granite and analyzed several relationships proposed by other researchers based on these data, such as the correlation between mineral content, grain size, mineral hardness, and rock strength. They pointed out that many of the correlations presented in the literature-such as the relationship between mica grain size and strength, and the ratio of quartz to feldspar and strength-seem to exhibit spurious correlations when a broader data set is considered. The study suggests that the correlations between different parameters may be caused by an unknown third variable (confounding variable), which could be related to both the independent and dependent variables.

In addition, existing laboratory experiments on the effect of quartz content on rock mechanical

behavior generally do not consider the role of grain heterogeneity. As pointed out by Sajid et al. (2016) and Hemmati et al. (2020), the strength of crystalline rocks is not only related to mineral content but also closely linked to the heterogeneity of the grains. In the discussion section of our study, we also show that the impact of mineral content on rock strength is generally smaller than the effects of grain heterogeneity and grain size.

In addition to the aforementioned points, we believe that the discrepancy between the numerical simulation and experimental results regarding the relationship between quartz content and peak strength is also related to misunderstandings in determining the grain boundary mechanical parameters in the GBM model.

5 The effect of heterogeneity on the thermal damage of crystalline rocks

The effect of temperature on the mechanical properties of rocks includes thermal cracking at particle-particle and particle-bond boundaries caused by thermal stress, the opening and closing of pre-existing microcracks due to thermal stress, and the fracturing of mineral crystal particles. The formation of thermally induced cracks marks the early stages of the degradation of the mechanical properties of crystalline rocks (Dang et al. 2023c). Therefore, it is essential to analyze the evolution of thermally induced cracks and thermal stress within rocks under the influence of temperature.

5.1 The effect of grain size heterogeneity on the thermal damage

5.1.1 Thermal crack distribution at different grain size heterogeneity

Figure 20 shows the thermally induced cracks within samples with heterogeneity index of 0.17 and 0.92 after different thermal treatments. Black lines represent intergranular cracks, while red lines indicate intragranular cracks. When the temperature is below 450°C, the number of thermally induced cracks within the samples is generally low. Most cracks are intergranular, mainly caused by differences in minerals' thermal expansion coefficients. Minerals like quartz, K-feldspar, and plagioclase maintain crystal structure stability without significant phase transitions or chemical decomposition within this temperature range. As a result, the number and scale of thermally induced cracks are limited, and crack propagation is relatively restrained. Since the thermally induced cracks are primarily intergranular, their weakening effect on the overall structure is relatively minor. Intergranular cracks do not significantly reduce the overall strength, as these cracks have not yet penetrated the grain interiors or caused ongoing damage. As shown in Fig. 10, the peak strength of the samples varies only slightly within the room temperature to 450°C, indicating that thermal treatment has a limited effect on the overall strength.

Figure 21 provides a statistical summary of the number of thermally induced cracks with different heterogeneity index. In any model, intergranular cracks consistently dominate. Intergranular cracks increase significantly at 600°C, while intragranular cracks surge dramatically at 900°C. For models with heterogeneity index of 0.17 and 0.92, the intergranular cracks increased by 4.26 times and 3.49 times from 450°C to 600°C, respectively. At 600°C, the thermal expansion differences between various minerals become significantly more pronounced, leading to substantial thermal stress at mineral grain interfaces and the formation of more intergranular cracks. Additionally, the α-β phase transition of quartz at 573°C, accompanied by volume changes and lattice reorganization, generates additional stress and cracks at the grain boundaries. This phase transition effect is significantly enhanced at 600°C, sharply increasing intergranular cracks. High temperatures also weaken the bonding strength at mineral boundaries, making intergranular cracks more likely to form and propagate. These findings are consistent with the results of Nasseri et al. (2007).

At high temperatures, mineral thermodynamic stability decreases, causing partial melting, decomposition, or lattice reorganization in some minerals. Structural instability triggers stress concentration within grains, leading to a sharp increase in intragranular cracks. From 750°C to 900°C, intragranular cracks increased by 6.49 times and 5.71 times, respectively. As the temperature rises to 900°C, the differences in thermal expansion become even more pronounced, making thermal stress concentration within the

minerals more significant. This stress induces crack propagation within the grains, resulting in many intragranular cracks.

The heterogeneity index increases the number of thermally induced cracks. As the heterogeneity index rises, mineral size differences become more pronounced, causing greater thermal stress concentrations and increasing the number of cracks. Greater heterogeneity increases irregularity at grain boundaries, making them more prone to stress concentration and crack formation. The more interfaces there are, the more pronounced the thermal stress concentration effect becomes, leading to more thermally induced cracks.

5.1.2 *Thermal stress analysis at different grain size heterogeneity*

Figure 22 shows the average contact force in different heterogeneity models during thermal treatment. The average contact force increases with temperature. Samples with uniform grain size distribution (H=0 and H=0.17) show greater average contact force than models with larger grain size differences. In uniform grain size samples, stress is more evenly distributed, leading to a higher contact force. Uniformly distributed grains can disperse and transmit stress more evenly, reducing the likelihood of local stress concentration and potential localized failure. The thermal expansion disparity between large and small grains is more pronounced in models with larger grain size differences, leading to stress concentration areas. This stress concentration can increase the contact force in local regions but results in an uneven overall distribution of contact force. Localized stress concentration may reduce the contact force between smaller grains, lowering the average contact force. From the perspective of force transmission, the force transmission paths in models with significant grain size differences are discontinuous, reducing overall stress transmission efficiency. The uneven force transmission between large and small grains results in a lower average contact force.

In Figure 22, the average contact force in the model with a heterogeneity index of 0.42 is lower than in models with heterogeneity index of 0.69 and 0.92. This indicates that the thermal stress after heating is influenced by differences in grain size and the shape and distribution of minerals. In models with higher heterogeneity (H=0.69 and H=0.92), more irregular mineral shapes lead to increased stress concentration and higher maximum contact forces. Irregular mineral particles with sharp corners and edges are more likely to become stress concentration points under thermal stress, increasing local stress (Dang et al. 2024a). This “sharp corner effect" is more pronounced in more heterogeneous models.

The distribution of minerals influences the stress transmission paths, thereby affecting crystalline rock’s thermodynamic response and failure mechanisms. A more uniform arrangement helps to evenly distribute stress, while an uneven distribution may lead to stress concentration. In models with higher heterogeneity, the mineral particles are arranged more irregularly, with complex and irregular interfaces between them (interface effect). This complicates the stress transmission paths and increases stress concentration at the interfaces, leading to higher maximum contact forces.

The evolution of thermal stress in two regions of the model was monitored for further analysis of the thermal stress distribution during thermal treatment. The measurement circles had a radius of 10 mm, with Measurement Circle 1 at the center in the positive x-axis direction and Measurement Circle 2 at the center in the negative x-axis direction.

Figure 23 shows the evolution of thermal stress in different grain size heterogeneity models during thermal treatment, with all thermal stress in the figure being compressive stress. Thermal stress evolution with temperature in various regions can be divided into three stages: (1) 150–450°C: Stable growth period. The thermal expansion of different minerals gradually leads to the accumulation of thermal stress, which increases almost linearly with temperature. (2) 450–600°C: Rapid growth period. Quartz undergoes an α-β phase transition at 573°C; the volume change and structural reorganization during this transition significantly affect the thermal stress distribution among mineral particles, leading to rapid growth in thermal stress. (3) 600–900°C: Slow growth period. Although the temperature continues to rise, the significant structural reorganization caused by the phase transition has already been completed. The appearance of cracks and pores slows the accumulation of thermal stress and provides pathways to relieve stress concentration, resulting in a slower rate of thermal stress increase.

Figure 23a shows that the model with a heterogeneity index of 0.69 consistently exhibits the highest thermal stress. In contrast, the model with a heterogeneity index of 0.42 consistently shows the lowest thermal stress. Assuming the differences in mineral thermal expansion coefficients are not considered, the larger the average grain size in a local region, the greater the thermal stress. In contrast, in the model with a heterogeneity index of 0.42, the mineral particles are more uniform in size and distribution, with the smallest average grain size allowing thermal stress to be more evenly distributed and reducing local stress concentration. Therefore, the overall thermal stress level in this model is lower. As shown in Fig. 5, the models with heterogeneity index of 0.69 and 0.92 still have larger average grain sizes within Measurement Circle 2. In contrast, the model with a heterogeneity index 0.42 has slightly larger average grain sizes within Measurement Circle 2. Grain size differences within the measurement circles across the models have decreased. Thus, thermal stress differences within Measurement Circle 2 are primarily due to varying mineral contents with significantly different thermal expansion coefficients.

Take the heterogeneity index of 0 and 0.17 as examples. In the model with a heterogeneity index of 0, the minerals within Measurement Circle 2 primarily comprise plagioclase and biotite. In contrast, in the model with a heterogeneity index of 0.17, the minerals within Measurement Circle 2 mainly comprise plagioclase, biotite, and quartz. The greater thermal expansion differences among the minerals in Measurement Circle 2 result in higher average thermal stress in the model with a heterogeneity index of 0.17 than in the model with a heterogeneity index of 0. The thermal expansion coefficients of different minerals determine the degree of their volume change during heating. Biotite has the lowest thermal expansion coefficient, plagioclase has a moderate coefficient, and quartz has the highest thermal expansion coefficient. When plagioclase, biotite, and quartz are combined, the significant differences in their thermal expansion lead to pronounced thermal stress concentrations at the mineral boundaries, resulting in higher thermal stress. In contrast, regions composed of plagioclase and biotite, which have more similar thermal expansion coefficients, experience fewer instances of thermal stress concentration during thermal treatment. The more consistent thermal expansion behavior between these two minerals reduces thermal stress concentration, leading to a lower average thermal stress within Measurement Circle 2.

5.2 The effect of grain size on the thermal damage

5.2.1 Thermal crack distribution at different grain size

Figure 24 shows the distribution of thermally induced cracks with grain sizes of 1.0 mm and 2.0 mm after thermal treatment. Figure 25 provides a count of thermally induced cracks. Below 450°C, the crack distribution varies significantly between samples with different grain sizes. In the 1.0 mm grain size sample, 169 intergranular cracks were observed, with no intragranular cracks detected. In the 2.0 mm grain size sample, there were 91 intergranular cracks and no intragranular cracks. Intergranular cracks showed an explosive increase between 450°C and 600°C, marking this range as critical for their expansion. Intrgranular cracks' explosive growth mainly occurs in the temperature range of 750°C to 900°C, indicating that higher temperatures significantly influence the formation and expansion of intragranular cracks. Taking the sample with a grain size of 1.0 mm as an example, in the two temperatures mentioned above ranges, the number of intergranular and intragranular cracks increased by 4.68 times and 5.84 times, respectively.

As shown in Fig. 25, as grain size increases, the number of intergranular cracks decreases while the number of intragranular cracks increases. Furthermore, the total number of thermally induced cracks decreases as grain size increases, consistent with the findings of Dang et al. (2024a). In larger grains, the relatively fewer grain boundaries mean fewer opportunities for thermal stress to concentrate at these boundaries, thereby reducing the formation of intergranular cracks. However, larger grains have a greater internal volume, which allows internal stress to accumulate and concentrate during thermal expansion, as it cannot be relieved through the fewer grain boundaries. The internal stress concentration effect leads to the formation of more intragranular cracks. Smaller grains have more interfaces, which are prone to forming stress concentration points during thermal expansion, forming more intergranular cracks. At 900°C, the number of intergranular cracks in the model with

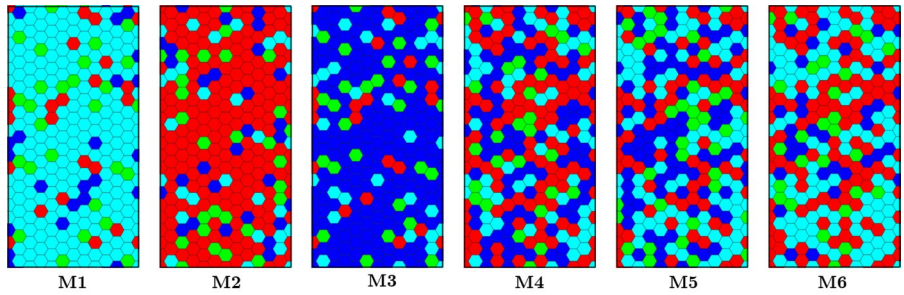

(a) Numerical model with mineral composition 1

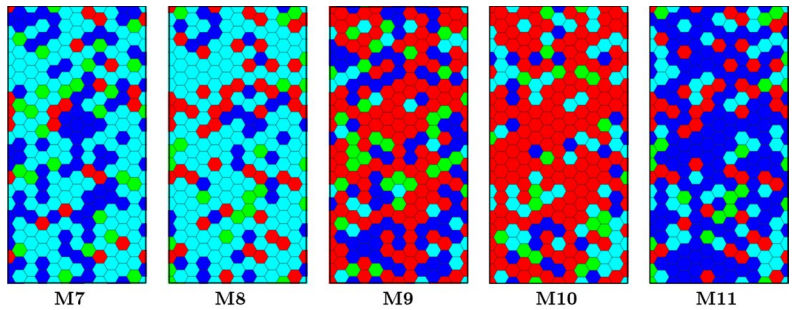

(b) Numerical model with mineral composition 2

Fig. 9 Numerical models with different mineral compositions

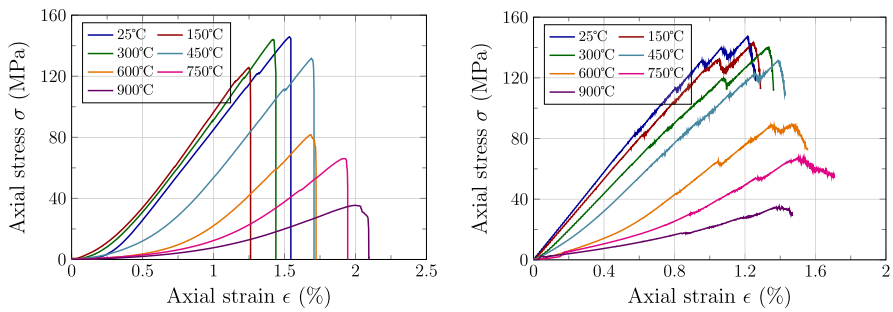

(a) Stress-strain curve of experimental

(b) Stress-strain curve of numerical

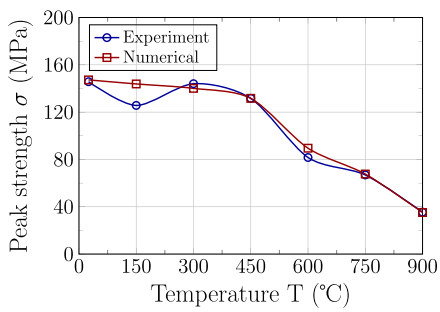

(c) Peak strength

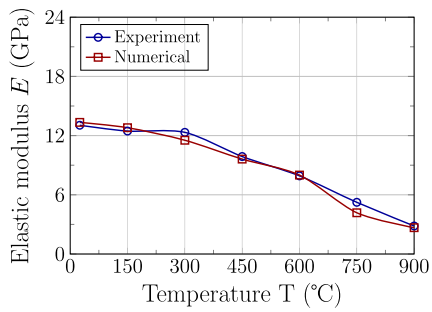

(d) Elastic modulus

Fig. 10 Comparison of experiment and numerical results

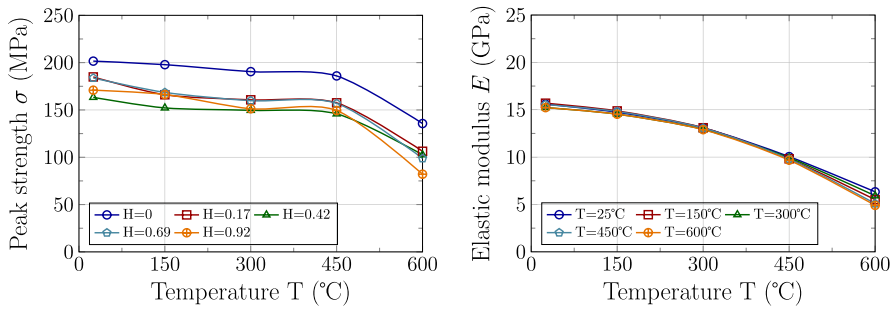

(a) Peak strength (b) Elastic modulus

Fig. 11 Peak strength and elastic modulus of samples at different thermal treatment temperatures

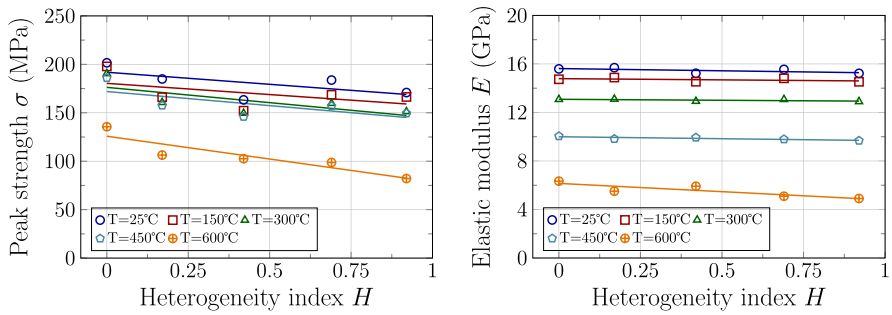

(a) Peak strength (b) Elastic modulus

Fig. 12 Peak strength and elastic modulus of samples with different heterogeneity index

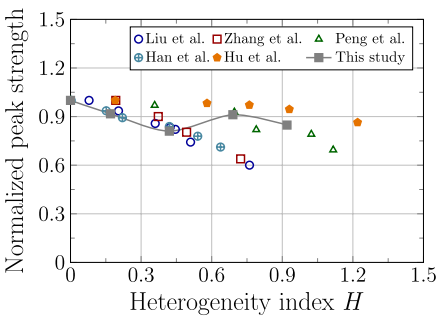

Fig. 13 Comparison between this article and literature on the relationship between grain size heterogeneity and strength

a grain size of 3.38 mm is 2.86 times that of intragranular cracks, whereas, in the model with a grain size of 1.0 mm, the number of intergranular cracks is 35.22 times that of intragranular cracks. Although intragranular cracks increase with grain size, the substantial reduction in intergranular cracks results in an overall decrease in the total number of cracks.

5.2.2 *Thermal stress analysis at different grain size*

Figure 26 shows the average contact force in models with different grain sizes. Overall, the average contact force increases with the thermal treatment temperature and grain size. Due to their larger volume and relatively fewer boundaries, larger grains are more prone to significant stress concentration during phase transitions and melting, resulting in greater contact forces with larger grain sizes than those with smaller grain sizes. The evolution of the average contact force can also be divided into three stages, consistent with those described in Sect. 4.1.2. This indicates that the evolution of thermal stress is solely related to temperature and is independent of grain size heterogeneity and grain size.

Figure 27 shows the evolution of thermal stress in the model's local regions during thermal treatment. Unlike in heterogeneous models, the grain sizes in models with different grain sizes are consistent, eliminating the potential complex effects of grain

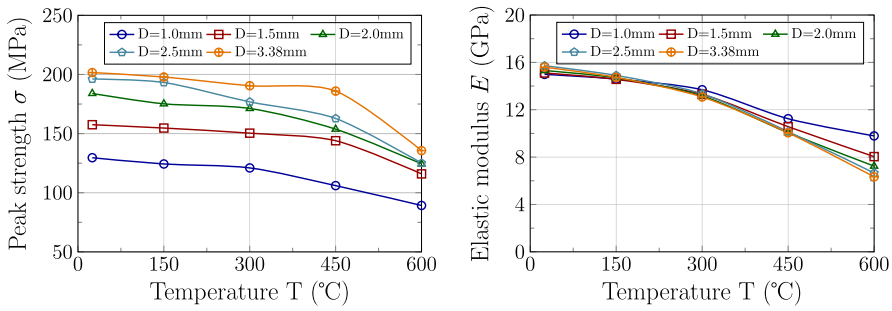

(a) Peak strength (b) Elastic modulus

Fig. 14 Peak strength and elastic modulus of samples at different thermal treatment temperatures

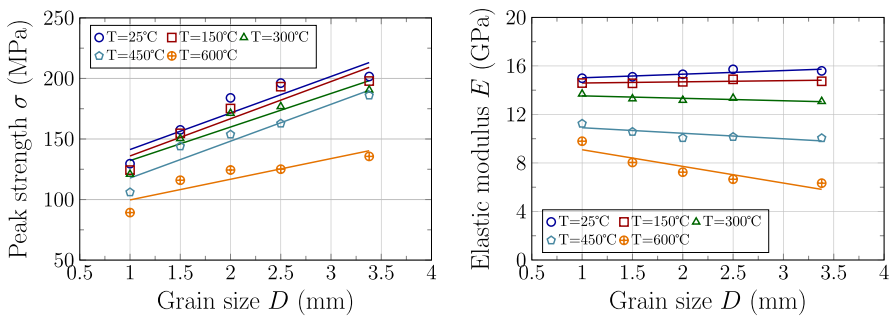

(a) Peak strength (b) Elastic modulus

Fig. 15 Peak strength and elastic modulus of samples at different thermal treatment temperatures

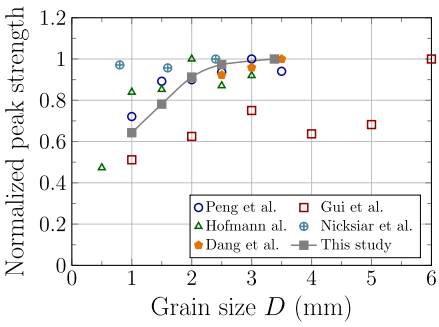

Fig. 16 Comparison between this article and literature on the relationship between grain size and strength

size heterogeneity. The data in Fig. 27 indicate that in Measurement Circle 1, thermal stress in each model is positively correlated with grain size. The larger the grain size, the higher the corresponding thermal stress.

At different thermal treatment temperatures, the thermal stress in Measurement Circle 2 of the sample with a grain size of 2.0 mm is consistently higher than that in the sample with a grain size of 2.5 mm. As observed in Fig. 9, the primary mineral composition within Measurement Circle 2 of the 2.0 mm grain size model includes K-feldspar, plagioclase, and biotite. At high temperatures, the stress concentration resulting from the thermal expansion of K-feldspar and plagioclase becomes more pronounced. The low expansion coefficient of biotite exacerbates this uneven expansion, leading to stress concentration at the interfaces and increasing the overall thermal stress. In the model with a grain size of 2.5 mm, Measurement Circle 2 primarily contains biotite and plagioclase. Although they have a thermal expansion coefficient difference, the absence of K-feldspar reduces the contribution of large thermal expansion differences. The expansion difference between plagioclase and biotite is smaller than that between K-feldspar and plagioclase, resulting in more uniform thermal expansion at high temperatures. This uniform expansion reduces uneven stress distribution, lowering overall thermal stress.

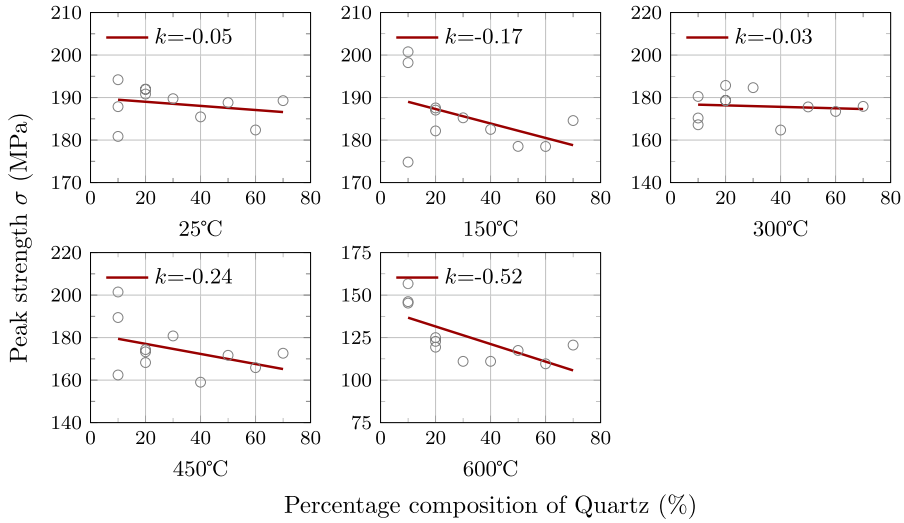

Fig. 17 The relationship between quartz content and peak strength after thermal treatment

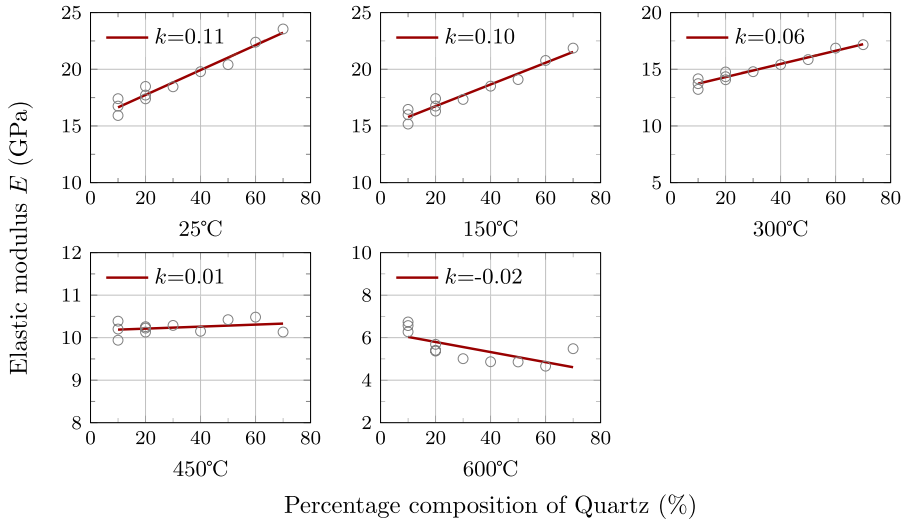

Fig. 18 The relationship between quartz content and elastic modulus after thermal treatment

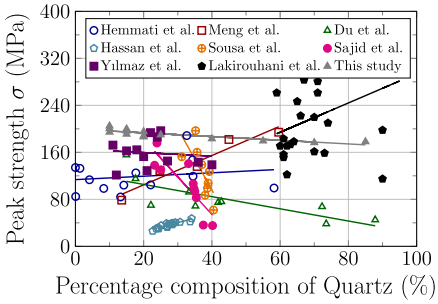

Fig. 19 Comparison between this article and literature on the relationship between quartz content and strength

5.3 The effect of quartz content on the thermal damage

As previously discussed, when grain size effects are excluded, thermal stress differences across regions are mainly due to the mineral composition in each area. These variations are primarily caused by differences in thermal expansion coefficients, thermal conductivity, and phase transition behavior of the minerals during heating. Next, the focus will shift away from the differences in grain size and their heterogeneous distribution to explore how different

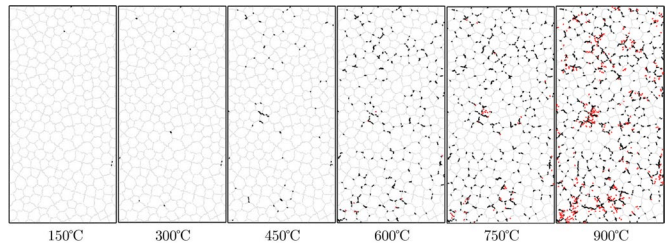

(a) Thermally induced cracks distribution for heterogeneity index of 0.17

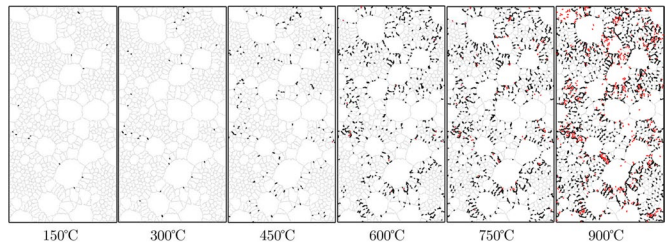

(b) Thermally induced cracks distribution for heterogeneity index of 0.92

Fig. 20 Thermally induced cracks in samples with different heterogeneity index after thermal treatment. Black lines represent intergranular cracks, while red lines indicate intragranular cracks

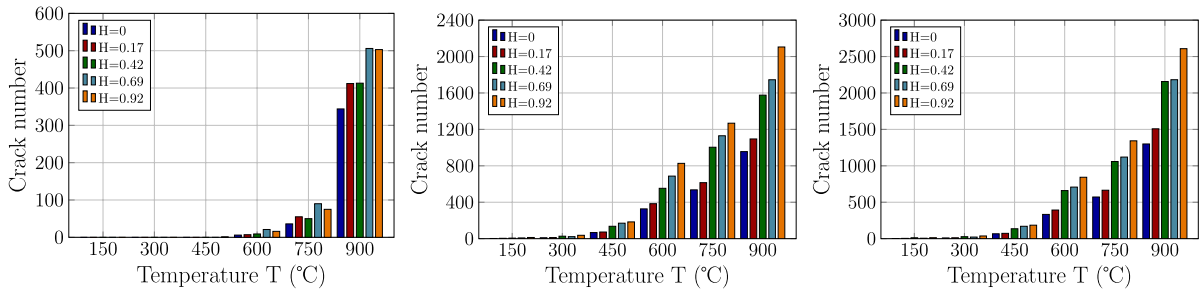

(a) Intragranular cracks (b) Intergranular cracks (c) Total number of cracks

Fig. 21 The number of thermally induced cracks with different heterogeneity index after thermal treatment

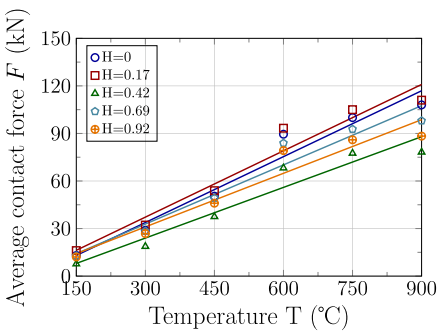

Fig. 22 Average contact force in different grain size heterogeneity models during thermal treatment

mineral compositions affect the thermal damage in crystalline rocks during thermal treatment.

The results in Figs. 17 and 18 do not fully capture the true impact of mineral content on the mechanical properties of the samples under varying temperatures. For example, the numerical models in Fig. 5 show that in M1, the quartz content is 70%, while the other three minerals each account for 10%. In M2 and M3, plagioclase and K-feldspar are the primary components, each at 70%, while the other minerals each account for 10%. In other models, the proportions of the other three minerals vary when the content of one mineral is the highest. This imbalance in mineral

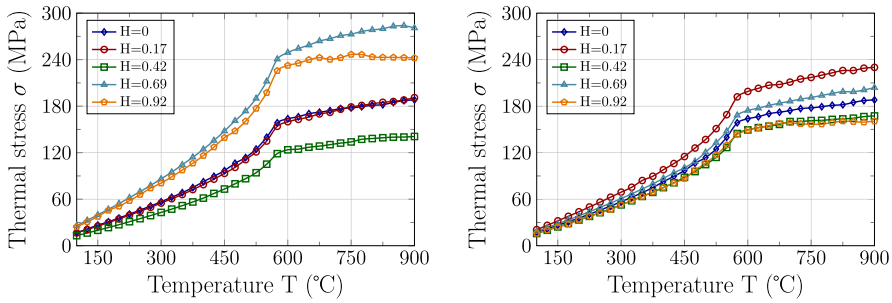

(a) Measure 1 (b) Measure 2

Fig. 23 Thermal stress evolution in local areas of model during thermal treatment

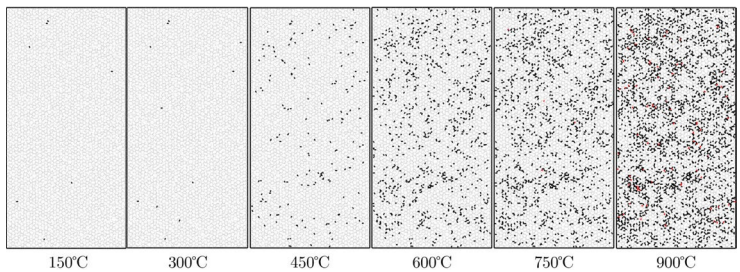

(a) Thermally induced cracks distribution for grain size of 1.0mm

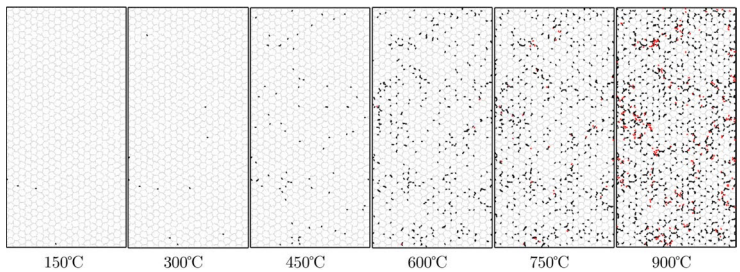

(b) Thermally induced cracks distribution for grain size of 2.0mm

Fig. 24 Thermally induced cracks in samples with different grain sizes after thermal treatment

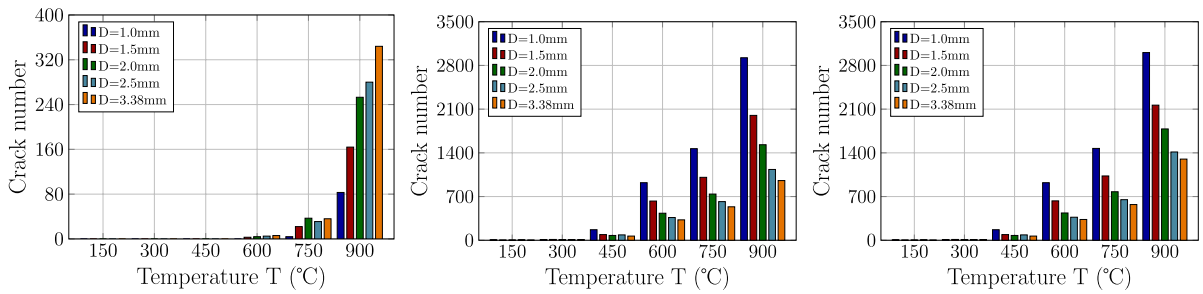

(a) Intragranular cracks (b) Intergranular cracks (c) Total number of cracks

Fig. 25 The number of thermally induced cracks in samples with different grain sizes after thermal treatment

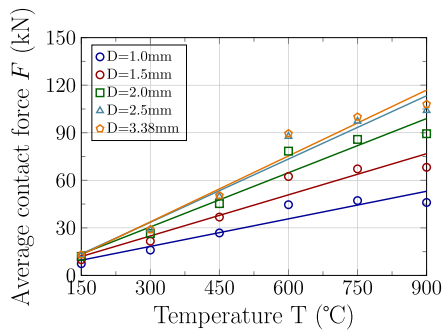

Fig. 26 Average contact force in different grain size models during thermal treatment

proportions makes it difficult to accurately understand how increased mineral content affects the thermodynamic behavior of samples under high-temperature conditions.

We designed a series of additional simulation scenarios to understand better how mineral composition affects the thermodynamic response of samples under high-temperature conditions. For example, in one scenario, if the quartz content is set to 25%, the other three minerals each account for 25%. If the quartz content increases to 55%, the other minerals are adjusted to 15% each. When the quartz content reaches 85%, the remaining minerals each make up 5%. While this approach may not perfectly reflect the mineral composition of certain crystalline rocks, it helps clarify how mineral composition influences the thermal damage and mechanical properties of crystalline rocks under high temperatures.

5.3.1 Thermal crack distribution at different quartz contents

Figures 28 and 29 illustrate the effect of quartz content on the distribution and quantity of thermally induced cracks during thermal treatment. Before 600°C, thermally induced cracks are predominantly intergranular, indicating that cracks mainly form along grain boundaries at lower temperatures. When the temperature exceeds 600°C, the type of thermally induced cracks changes significantly, with intragranular cracks becoming the predominant type.

As quartz content increases, the number of intragranular thermally induced cracks rises significantly. At 750°C, there is a positive correlation between the number of intragranular cracks and the quartz content. Specifically, when the quartz content is 25%, the number of intragranular cracks is 928, but this number increases to 1277 when the quartz content rises to 70%. This indicates that quartz's high thermal expansion coefficient leads to greater internal stress at higher temperatures, thereby promoting the formation of intragranular cracks. At 900°C, the increase in intragranular cracks becomes even more pronounced, indicating that high temperatures intensify the stress concentration caused by quartz. In models with quartz contents of 25, 40, 55, and 70%, the number of intragranular cracks increased by 0.82 times, 1.2 times, 1.63 times, and 2.34 times from 750°C to 900°C, respectively.

During thermal treatment, the relationship between the number of intergranular cracks and quartz content may not be clear because intergranular cracks are primarily influenced by the characteristics of mineral interfaces rather than solely determined by the quartz content. The formation of intergranular cracks results from the combined

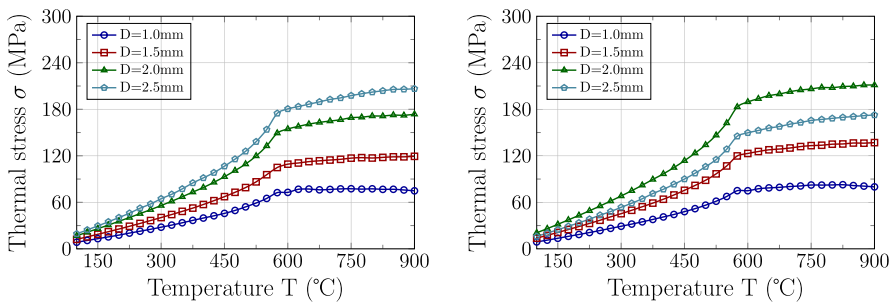

(a) Measure 1 (b) Measure 2

Fig. 27 Thermal stress evolution in local areas of model during thermal treatment

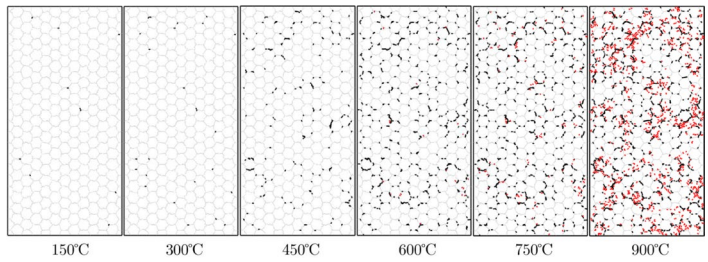

(a) Thermally induced cracks distribution for Quartz content of 25%

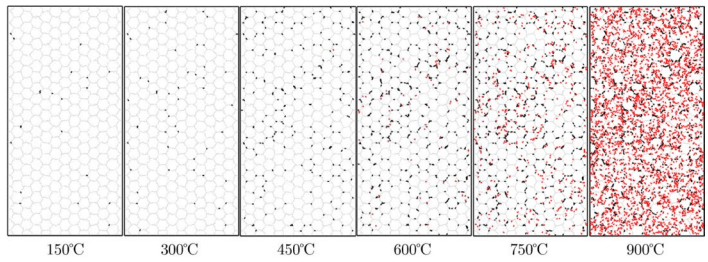

(b) Thermally induced cracks distribution for Quartz content of 70%

Fig. 28 Thermally induced cracks in samples with different quartz contents after thermal treatment

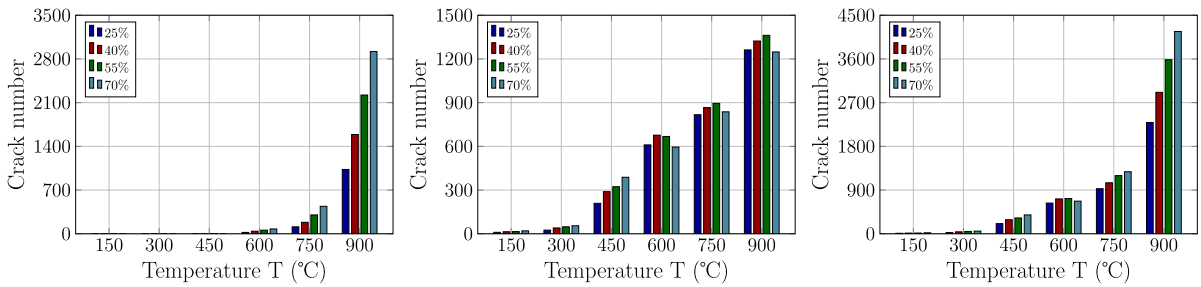

(a) Intragranular cracks (b) Intergranular cracks (c) Total number of cracks

Fig. 29 The number of thermally induced cracks in samples with different quartz content after thermal treatment

effects of different mineral interface properties. Quartz's high brittleness, thermal expansion coefficient, and more pronounced phase transition effects at high temperatures exacerbate stress concentration, leading to extensive formation of intragranular cracks.

5.3.2 Thermal stress analysis at different quartz contents

Figure 30a shows the average contact force in samples with different primary minerals, each with a mineral content of 55%. As seen in Fig. 30a, when the primary mineral content is 55%, the average contact force is related to the thermal expansion coefficient of the mineral. Specifically, the larger the thermal expansion coefficient of the primary mineral type, the greater the average contact force in the sample. For example, at 750°C, when the primary minerals are biotite, K-feldspar, plagioclase, and quartz, the average contact forces are 82.5 kN, 117 kN, 149 kN, and 232 kN, respectively. The increments in average contact force are 34.5 kN (from biotite to K-feldspar), 32 kN (from K-feldspar to plagioclase), and 83 kN (from plagioclase to quartz), showing a nonlinear growth trend.

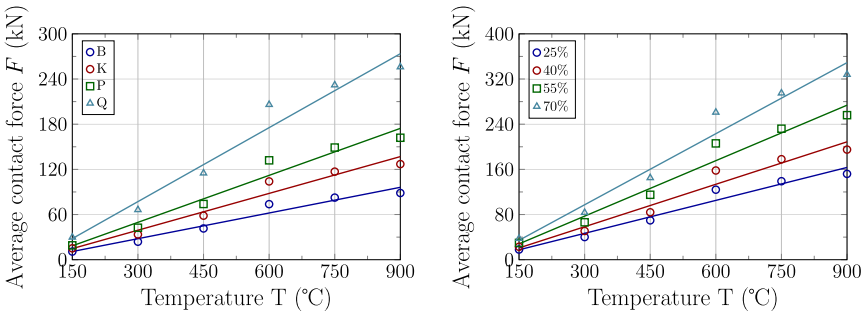

Fig. 30 Comparison of average contact force under different conditions

(a) Average contact force in samples with different primary minerals at 55% mineral content

(b) Average contact force in samples with different quartz contents

Figure 30b shows the average contact force in samples with varying quartz content. The average contact force increases with the quartz content. However, it is worth noting that with the increase in quartz content, the rise in average contact force becomes more pronounced. For example, at 750°C, as the quartz content increases from 25 to 70%, the average contact force increases by 39 kN, 54 kN and 63 kN, respectively. Quartz's high stiffness and strength contribute significantly to the mechanical performance of the overall structure, leading to a rapid increase in contact force with quartz content increases.

6 The effect of heterogeneity on the failure mechanism and microseismic behaviors in thermally treated crystalline rock

6.1 The effect of grain size heterogeneity on the failure mechanism and microseismic behavior

6.1.1 The distribution of cracks after loading

Figure 31 shows the distribution of microcracks after loading in different grain size heterogeneity models at room temperature. Black and red represent intergranular tensile and shear cracks, respectively, while blue and magenta represent intragranular tensile and shear cracks. From the distribution of microcracks, it can be observed that most microcracks extend and propagate along the axial direction, forming axial intergranular tensile and shear cracks, with fewer intragranular cracks present. Fractures in brittle rocks typically occur along grain boundaries parallel to the direction of the maximum principal stress. Since grain boundaries are the weakest points in the mechanical structure of the sample, fractures along these boundaries are more likely to occur than intragranular fractures. This failure mode manifests as axial splitting both microscopically and macroscopically, with cracks primarily propagating along the length of the rock, consistent with the observations in the literature (Ma et al. 2024; Wang et al. 2022; Zhou et al. 2024; Potyondy 2010), as shown in Fig. 32.

As shown in Fig. 11, the peak strength of the sample with a heterogeneity index of 0 is significantly higher than that of the other samples. This indicates that a uniform grain size distribution generally

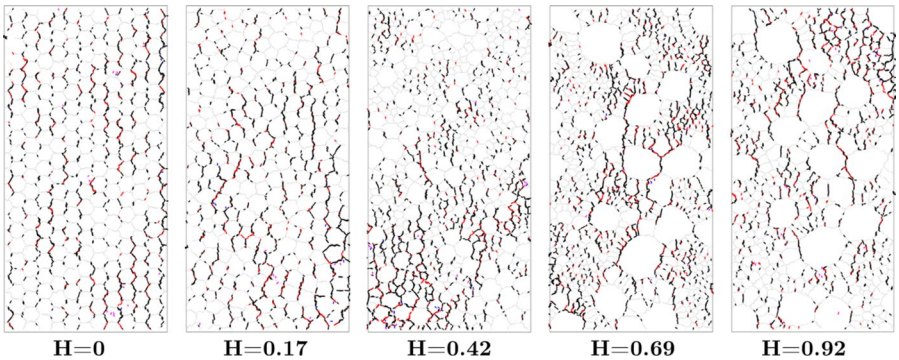

Fig. 31 Distribution of microcracks after loading in different grain size heterogeneity samples at room temperature

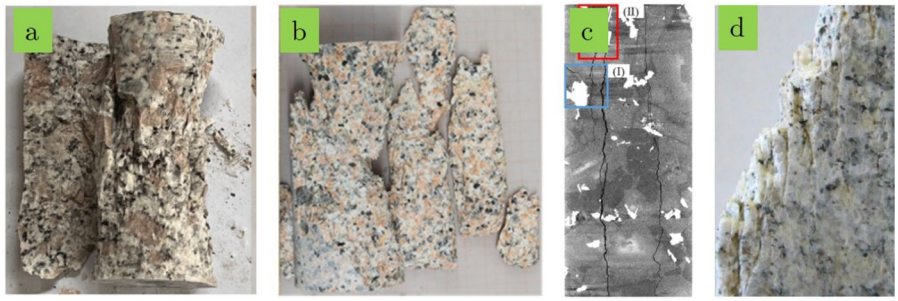

Fig. 32 The uniaxial compression failure modes of crystalline rocks observed in the laboratory. The sample fractures primarily develop along the loading direction, forming axially aligned cracks. Modified from **a** Ma et al. (2024), **b** Wang et al. (2022), **c** Zhou et al. (2024), **d** Potyondy (2010)

enhances the material's overall mechanical performance and toughness. The increased toughness delays the initial formation of cracks and raises the energy required for cracks to reach critical propagation, thereby reducing the probability of macroscopic fracture in the sample. This observation is consistent with the findings reported in the literature (Peng et al. 2017a, 2021).

Taking the sample with a heterogeneity index of 0 as an example and referring to Fig. 5, it can be observed that grain boundary cracks tend to appear at the interfaces between different minerals, especially at grain boundaries where there is a significant thermal expansion coefficient difference. Additionally, grain boundaries of the same mineral with weaker strength are more prone to microcrack formation. In contrast, grain boundaries of the same mineral with greater strength are less likely to develop microcracks. Ignoring the effects of grain shape and size, interfaces between minerals with significantly different strengths become potential stress concentration zones. Under external force, a mineral with lower strength may be unable to withstand the same stress level as a stronger mineral, leading to stress concentration at the interface, which promotes crack formation and propagation. For example, if a grain boundary consists of high-hardness quartz and low-hardness biotite, the quartz may transfer more stress to the biotite under external loads, causing the biotite to fracture. In the case of grain boundaries within the same mineral, when the mineral has high strength, the structural integrity of the grain boundary can resist a certain stress level. Even if a few cracks form locally, the surrounding high-strength structure can prevent further crack propagation, acting as a "crack-stopper". When the minerals on both sides of a grain boundary have lower strength, the boundary is more likely to fracture under external force, forming microcracks. In this study, a Weibull distribution was used to account for the effects of natural defects and the heterogeneity of material strength distribution. Ignoring the impact of the aforementioned geometric heterogeneity, areas where microcracks accumulate may also correspond to regions with defects or weaker mechanical properties.

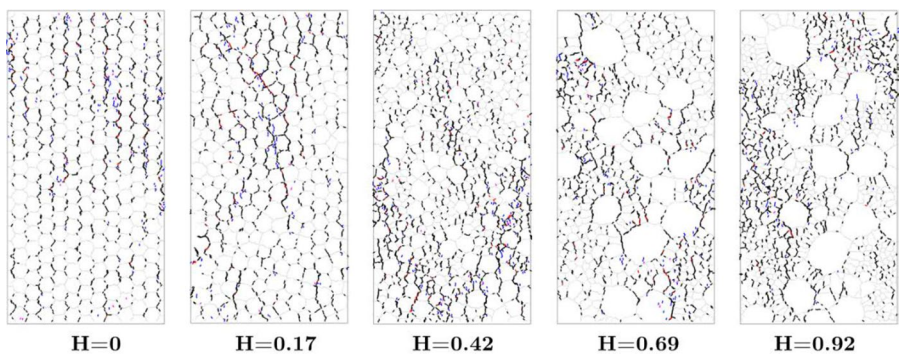

Fig. 33 Microcrack distribution after loading in samples with different grain size heterogeneity at 600°C treatment

Figure 33 shows the distribution of microcracks after loading at 600°C. The distribution of microcracks indicates a significant increase in intragranular cracks in different grain size heterogeneity models after the 600°C treatment. While intragranular cracks increase in high-temperature samples, they rarely form inside large grains. These cracks mostly form in weaker minerals or smaller grains. Grain boundaries, acting as natural barriers within the crystal structure, impede the propagation of cracks. After forming, cracks may propagate along the path of least resistance, depending on the distribution of grain boundaries and the grain size. In smaller grains with dense boundaries, cracks face less resistance, allowing them to extend along boundaries or within weakened grains. In contrast, in larger grains, where grain boundaries are fewer, cracks are more difficult to penetrate, resulting in fewer intragranular cracks within large grains.

Intragranular cracks typically occur when the internal stress within the material exceeds the tensile strength of the grain itself. Under the influence of temperature, the crystal structure may become more brittle, making the grains more susceptible to cracking under internal stress. Additionally, high temperatures generate more defects within the sample, which become sources of stress concentration under external loads. Once a crack initiates, it can easily propagate through these defect sites. Grain boundaries and crystal strength weaken due to high temperatures, reducing the fracture toughness of the grains. As the cracks propagate, initial microcracks can develop into macroscopically visible fractures. This process involves the transition of cracks from the grain boundary to the interior of the grain, particularly when there are significant structural or mechanical weaknesses within the grain. These factors collectively lead to a substantial increase in intragranular cracks.

6.1.2 *The influence of grain size heterogeneity on the AE magnitude and frequency*

Based on the moment tensor inversion theory, this study established a method for simulating AE events during rock failure at the microscale. This method can simultaneously provide characteristics such as AE events' time, location, and rupture strength. The specific process for simulating AE based on the moment tensor inversion theory in PFC is detailed in the literature (Dang et al. 2023a).

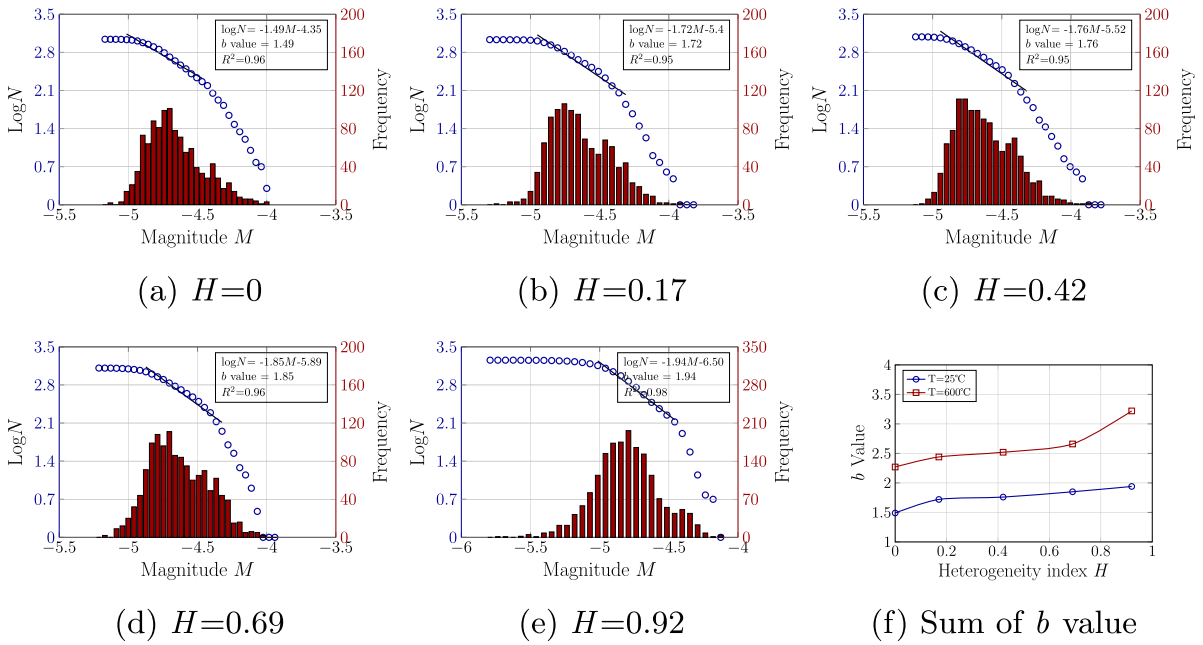

Fig. 34 The relationship between AE magnitude, number, and frequency in samples with different grain size heterogeneity index

Figure 34a, e shows the relationship between the magnitude, frequency, and number of AE events with different grain size heterogeneity index. The relationship between AE magnitude and frequency exhibits a normal distribution, while the relationship between AE magnitude and number follows a power-law distribution. In all grain size heterogeneity models, the AE magnitude is primarily concentrated between −5.0 and −4.5. Notably, when the magnitude is −4.75, the frequency of AE events peaks, a phenomenon that is independent of grain size distribution heterogeneity. The number of AE events gradually decreases when the magnitude is greater or less than −4.75. As the AE magnitude increases, the number of AE events sharply declines, and eventually, the slope of the AE event count curve transitions to 0. Gutenberg (2013) proposed a relationship between earthquake magnitude and frequency by studying the characteristics of global earthquake activity. This relationship allows for further analysis of AE magnitude:

$$\mathrm{Log}N = a - bM \tag{11}$$

Where N is the cumulative number of AE events with magnitudes greater than N, a and b are constants. The variation in the b value is one of the precursors of rock fracture. It holds significant physical meaning, reflecting the ratio of small to large AE events during the rock fracture. A high b value indicates a greater number of low-magnitude AE events and fewer high-magnitude AE events, while a low b value indicates the opposite. The b value reveals changes in the average stress and internal strength of the rock over time and reflects the scale of microcracks within the rock. The b value is widely used to characterize the development of microcracks within the rock. By performing linear fitting on the stages of rapid change in the number of AE events shown in Fig. 34a, e, the b value can be determined.

Figure 34f summarizes the b values for samples with different grain size heterogeneity index at room temperature and after 600°C treatment.As the heterogeneity index increases, the b value also increases. Additionally, the b value of the samples after high-temperature treatment is higher than that of the samples at room temperature during failure. Notably, the b value exhibits a more significant increase for the high-temperature treated samples with a high grain size heterogeneity index. This indicates that both the grain size heterogeneity index and high-temperature treatment substantially affect the b value, with their combined effect being more pronounced at higher grain size heterogeneity index.

The grain size heterogeneity index measures the degree of non-uniformity within a material's internal composition or structure. The heterogeneity in grain size distribution leads to uneven stress distribution among grains of different sizes. The higher grain boundary density in regions with smaller grains results in a more pronounced stress concentration. While larger grains may impede crack propagation, smaller grain regions allow cracks to spread more easily along these boundaries due to their dense grain boundaries. This phenomenon is more evident in rocks with a high heterogeneity index, where the significant difference in grain sizes makes cracks more likely to form and propagate in smaller grain regions. At room temperature, samples with a high heterogeneity index exhibit more significant stress concentration due to the large disparity in grain sizes, leading to frequent microcrack formation and higher AE b values.

High-temperature treatment induces numerous defects within crystalline rocks, significantly impacting AE events and their magnitudes during subsequent loading. After thermal treatment, the distribution of defects within the material becomes more widespread and denser, providing additional pathways for crack coalescence and propagation. During loading, the stress concentration at the crack tip drives the crack to propagate along the path of least resistance, where pre-existing microcracks can easily connect and merge under stress. Since defect regions already provide pathways for crack propagation, the cracks do not need much energy to form new fracture surfaces, making crack propagation easier. When cracks propagate along pre-existing cracks or paths formed during thermal treatment, the energy released is lower, leading to an increase in low-energy AE events. As the frequency of low-energy events and high-energy events decreases, the AE b value rises.

Figure 35 summarizes the relationship between AE magnitude and frequency in samples with different grain size heterogeneity index at room temperature and 600°C. At room temperature, the AE magnitudes with a heterogeneity index of 0.92 are generally lower than those in other samples, and they exhibit a greater

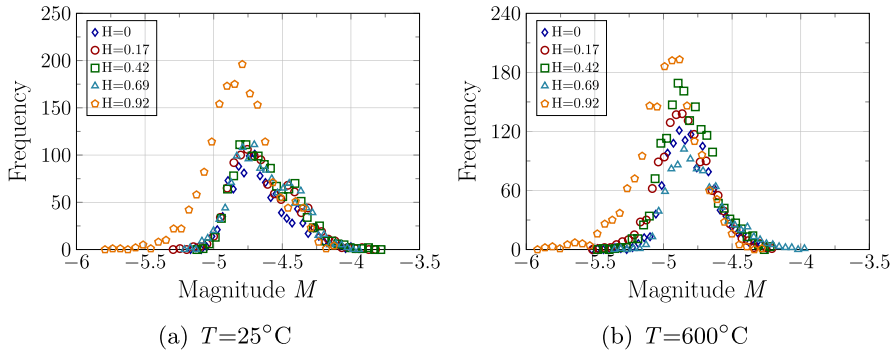

Fig. 35 The relationship between AE magnitude and frequency in samples with different grain size heterogeneity index at room temperature and after thermal treatment at 600°C

number of AE events. The magnitude distribution for the sample with a heterogeneity index of 0.92 ranges from −5.75 to −4.0, while other samples have magnitudes ranging from −5.25 to −3.75. At 600°C, the AE magnitude for the sample with a heterogeneity index of 0.92 ranges from −6.0 to −4.25, whereas other models range from −5.5 to −4.0. The high-temperature results in a uniform reduction in AE magnitudes during failure across all samples, indicating that the energy released during failure in high-temperature-treated samples is uniformly lower. This suggests that the material's overall strength decreases due to microstructural changes caused by high temperatures, making crack formation and propagation easier.

In highly heterogeneous rocks, the uneven stress distribution caused by differences in grain size may lead to more frequent AE events. Specifically, due to the significant size differences between grains, cracks may form and rapidly propagate along the edges of multiple small or large grains, triggering more AE events. Although the number of events is high, each event releases relatively low energy, as cracks are often "intercepted" by adjacent grains as they form. This interception limits further crack propagation, resulting in shorter crack paths and indirectly reducing the likelihood of cracks merging and forming large-magnitude events. The pronounced discontinuity between grains creates more complex and variable crack propagation paths in highly heterogeneous crystalline rocks. Large grains may inhibit further crack propagation, while small grains may fracture under lower stress. This interaction between large and small grains creates intricate crack paths, contributing to more low-magnitude AE events.

6.2 The effect of grain size on the failure mechanism and microseismic behavior

6.2.1 The distribution of cracks after loading

Figure 36 shows the crack distribution after loading in different grain size models at room temperature. To eliminate the interference of grain size distribution and shape on the analysis, the grain size and shape were kept consistent across all models. Like samples with different grain size heterogeneity index, the primary cracks formed during failure were intergranular tensile cracks and a few intergranular shear cracks, with intragranular cracks relatively rare. All

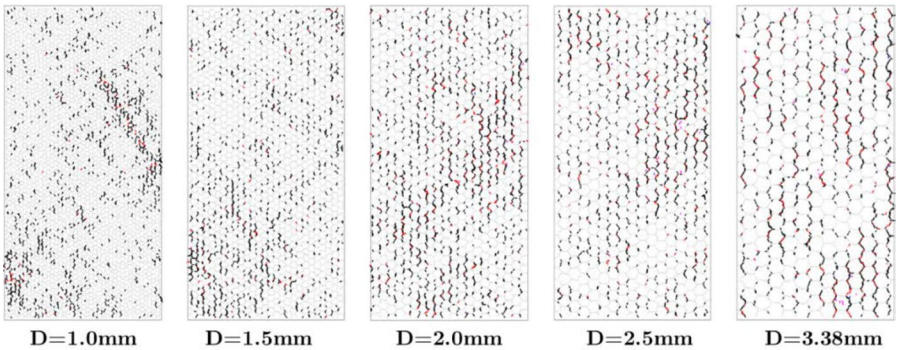

Fig. 36 Microcrack distribution after loading in samples with different grain size at room temperature

microcracks originated at the grain boundaries. In the large grain size model, microcracks primarily formed parallel to the maximum principal stress direction. They propagated along this direction, with no macroscopic cracks observed in this model. In contrast, although microcracks in the small grain size model also primarily form intergranularly, these cracks have the potential to merge and develop into macroscopic fractures. Unlike the large grain size model, the intergranular cracks in the small grain size samples not only propagate along the direction of the maximum principal stress but can also combine with surrounding cracks to form diagonal.

In the large grain size model, cracks primarily form at the grain boundaries and propagate along the direction of the maximum principal stress. This mode of crack formation indicates that large grains provide longer, straight paths, allowing cracks to extend continuously along the stress direction without interruption. Additionally, due to the fewer grain boundaries in large grains, the likelihood of crack coalescence at the boundaries is reduced, and crack propagation is more likely to be obstructed, making macroscopic cracks less likely to form. In contrast, the small grain size model exhibits different crack behavior, primarily because the greater number of grain boundaries in small grains increases the chances of cracks not only forming along the direction of maximum principal stress but also intersecting and merging with cracks from other directions, potentially leading to diagonal or complex macroscopic fractures.

The dense distribution of grain boundaries in the small grain size samples facilitates crack interaction and coalescence in multiple directions, increasing the likelihood of macroscopic crack formation. Microcracks primarily accumulate at the grain boundaries between two minerals with significant strength differences and at the interfaces between biotite grains. This is mainly due to stress concentration caused by strength differences, which often occur at grain boundaries where the mineral's elastic modulus or thermal expansion coefficients differ significantly. These boundaries cannot effectively accommodate the deformation of different minerals during stress transfer, leading to the formation of microcracks at the interfaces.

Figure 37 shows the distribution of microcracks in samples after loading at thermal treatment 600°C. Compared to the samples at room temperature, the number of microcracks of all types has significantly increased in the heat-treated samples. Although intergranular cracks remain the predominant type, macroscopic fracture zones can be observed in all heat-treated samples. Due to the significant increase in microcracks, these cracks are more likely to connect, forming larger crack networks that eventually develop into macroscopic fractures. High-temperature treatment can lead to material embrittlement, especially when it weakens grain boundaries or causes mineral phase changes. This embrittled material is more prone to fracturing under relatively low stress. Consequently, macroscopic fracture surfaces are greater in heat-treated samples than at room temperature.

6.2.2 *The influence of grain size on the AE magnitude and frequency*

Figure 38a, e illustrate the relationship between AE event magnitude, frequency, and number in different grain size models at room temperature. Figure 38f summarizes the AE *b* values for different grain size models at room temperature and after thermal treatment at 600°C. For samples with varying grain sizes, the number of AE events peaks around a magnitude

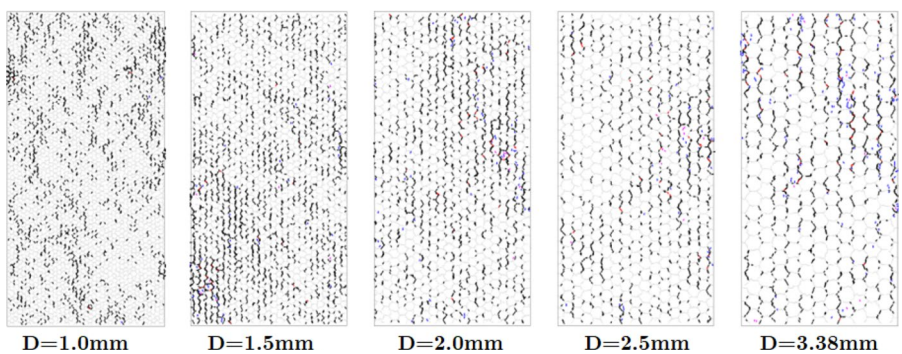

Fig. 37 Microcrack distribution in different grain size models after loading at 600°C thermal treatment temperature

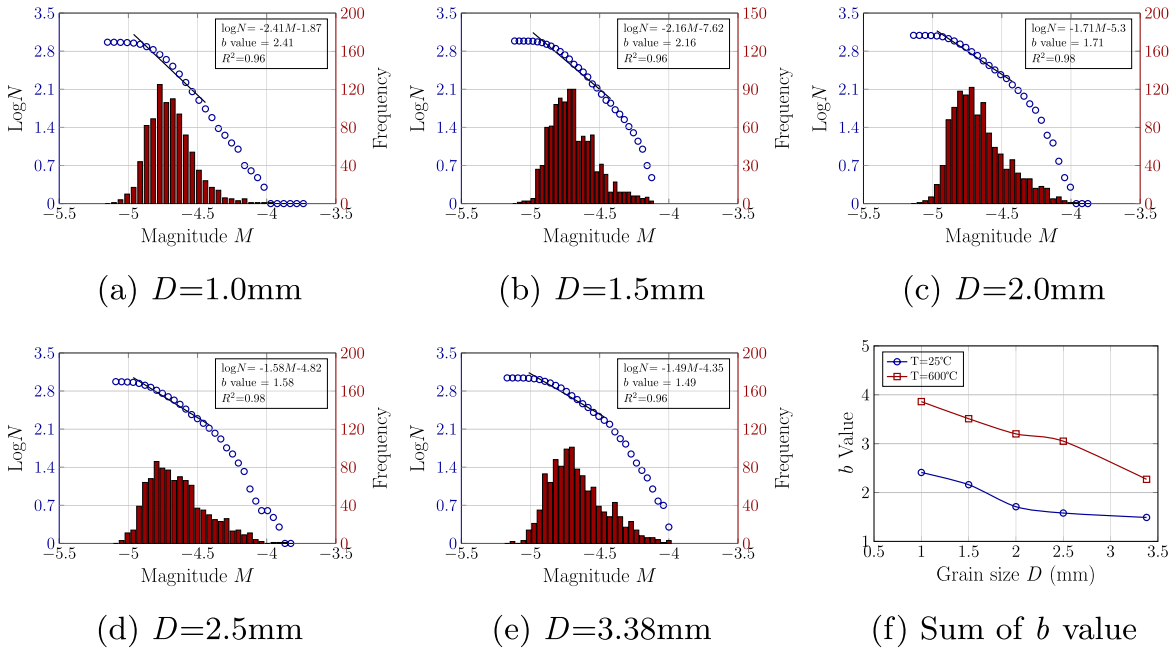

Fig. 38 The relationship between AE magnitude, number, and frequency in samples with different grain size

of −4.75, with the frequency of AE events gradually decreasing for magnitudes greater and smaller than −4.75.

For the different grain size models, AE event magnitudes are primarily distributed between −5.2 and −3.75, with most AE events concentrated between −4.8 and −4.5. Figure 38f shows that, compared to the *b* values of samples with varying grain size heterogeneity index (Fig. 34), the increase in *b* values after 600°C treatment is significantly greater in the different grain size models. Whether the samples were at room temperature or thermally treated, the AE *b* values decrease as the grain size increases. The number of grain boundaries in rocks with large grains is relatively low, meaning there is less resistance when cracks propagate. As a result, cracks can extend continuously over longer distances without many start-stop points, potentially leading to high-energy AE events. In contrast, materials with smaller grain sizes have more grain boundaries that can act as barriers to crack propagation. Cracks frequently initiate and stop over shorter distances, resulting in more low-energy AE events. Additionally, as observed in Figs. 36 and 37, small grains increase the complexity of crack paths, leading to more frequent reflection, twisting, or branching at grain boundaries. These activities are low in energy but high in frequency, contributing to higher *b* values.

Thermal treatment increases the number of microcracks within the material. The proliferation of microcracks means that cracks can propagate under lower loads, leading to numerous low-energy events. Smaller grains, with more grain boundaries, provide more sites for crack formation, potentially resulting in more frequent low-energy AE events. In contrast, larger grains may allow for larger cracks between grain boundaries. Still, these cracks tend to be more continuous due to the fewer boundaries, leading to fewer but higher-energy AE events.

Figure 39a, b illustrate the relationship between AE magnitude and frequency for samples with different grain sizes at room temperature and after thermal treatment. At room temperature, there is no significant difference in the maximum and minimum magnitudes across different grain sizes, and the peak frequency of AE events shows no clear correlation with grain size. However, after treatment at 600°C, the AE magnitude distribution range narrows from −5.2 to −3.75 at room temperature to −5.7 to −4.0.

Specifically, at room temperature, AE events are primarily concentrated between −4.75 and −3.75,

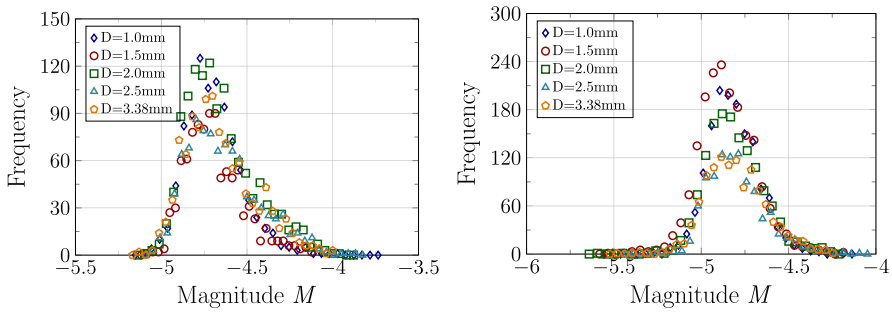

Fig. 39 The relationship between AE magnitude and frequency in samples with different grain size at room temperature and after thermal treatment at 600°C

while after thermal treatment, the distribution of AE events becomes more uniform. High-temperature treatment reduces the frequency of AE events and lowers the peak frequency of AE events in large grain size samples. In comparison, cracks in large grain size samples are more likely to form larger, continuous crack paths, unlike in small grain size samples where multiple independent small crack paths develop. The formation of these larger, continuous paths reduces the total frequency of crack formation, as once a larger crack is initiated, its propagation requires fewer activations, thereby decreasing the total number of AE events.

6.3 The effect of mineral composition on the microseismic

Figure 40 illustrates the relationship between AE magnitude and frequency for samples with varying biotite content at room temperature and after thermal treatment at 600°C. At room temperature, there is no significant correlation between AE magnitude and frequency across different biotite content samples, with the magnitude distribution ranging from −5.75 to −3.8. The AE event frequency peaks at a magnitude of −4.75. Figure 40 shows that the proportion of AE events at different magnitudes remains consistent across samples with varying biotite content. The presence of biotite does not directly influence the AE source mechanism. This may be because biotite's physical properties affect the speed and path of crack propagation, but they are not significant enough to alter the overall distribution of AE events. Figure 40b shows the relationship between AE magnitude and frequency for samples with varying biotite content at 600°C. Compared to room temperature, the overall AE magnitudes are lower, ranging from −6.0 to −4.2, with the frequency peaking at −4.9.

At 600°C, the overall AE event magnitudes decrease (ranging from -6 to −4.2), indicating that high-temperature treatment weakens the material's internal structural strength, making it easier for crack activity to occur at lower energy levels than at room temperature. The increase in low-magnitude AE events suggests that internal cracks form more readily under high-temperature conditions under lower

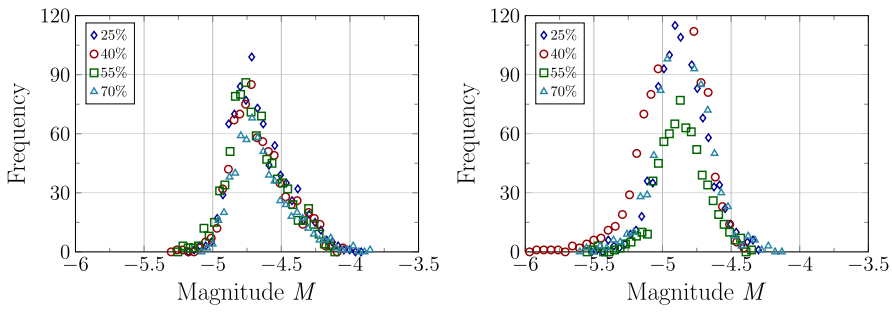

Fig. 40 The relationship between AE magnitude and frequency in samples with different biotite content at room temperature and after thermal treatment at 600°C

stress or energy conditions. Reduced medium and high-magnitude events may result from pre-existing defects post-thermal treatment, allowing cracks to initiate with less energy. High-temperature damage makes the material more brittle, lowering the energy needed for crack propagation. While crack initiation frequency rises, high-energy events decrease as cracks form and spread under smaller stress.

Figure 41 illustrates the relationship between AE magnitude and frequency in samples with varying quartz content at room temperature and after 600°C thermal treatment. At room temperature, the AE magnitude in samples with different quartz contents ranges from −5.2 to −3.9, showing a relatively narrow distribution compared to samples with varying biotite content. This suggests that quartz's high hardness and brittleness produce more concentrated energy during crack formation. Quartz's physical properties may cause cracks to be less likely to form until a certain energy threshold is reached. Still, once formed, they expand rapidly and releasing significant energy. The frequency of AE events peaks at a magnitude of −4.75, which represents the typical energy required for crack propagation in samples under general stress conditions. This magnitude may also indicate a critical point, suggesting that crack propagation in the sample is most active at this energy level. Cracks with magnitudes below this threshold are less likely to be detected, while AE events exceeding this magnitude may rapidly lead to sample failure.

For samples treated at 600°C, the AE magnitude distribution ranges from −5.5 to −4.2 for samples with 25, 40, and 55% quartz content, while for the sample with 70% quartz content, the distribution extends from −6.0 to −4.2. As the quartz content increases to 70%, the lower limit of the magnitude distribution expands to −6.0, indicating that AE events can occur even at lower energy levels. The high brittleness of quartz, exacerbated by thermal treatment, likely leads to the formation of more microcracks, which can trigger AE events at lower energy thresholds. Higher quartz content suggests that the material becomes more brittle after thermal treatment, making it more susceptible to fracturing and generating AE events under lower stress conditions.

For the samples treated at 600°C, the proportion of moderate-magnitude AE events decreases as the quartz content increases. Compared to samples with 60% quartz content, the proportion of high-magnitude AE events decreases by 5.6%, while the proportion of low-magnitude events increases by 16.42% in samples with 70% quartz content. This suggests that increased quartz content, particularly after high-temperature treatment, significantly influences the distribution of AE magnitudes in rock samples, indicating that the material's brittleness and crack sensitivity increase with higher quartz content. This effect is particularly pronounced when the quartz content reaches 70%, likely due to the material becoming more uniform in structure and more prone to brittleness (He et al. 2023).

Figure 42 shows the b value for samples with different contents of biotite and quartz. As the content of biotite in the sample increases, the b value gradually decreases. Conversely, as the content of quartz increases, the b value gradually increases. At room temperature, the b value is minimally affected by mineral content, resulting in relatively small variations in the b value.

However, when the thermal treatment temperature reaches 600°C, the changes in the b value become more pronounced. Under high-temperature

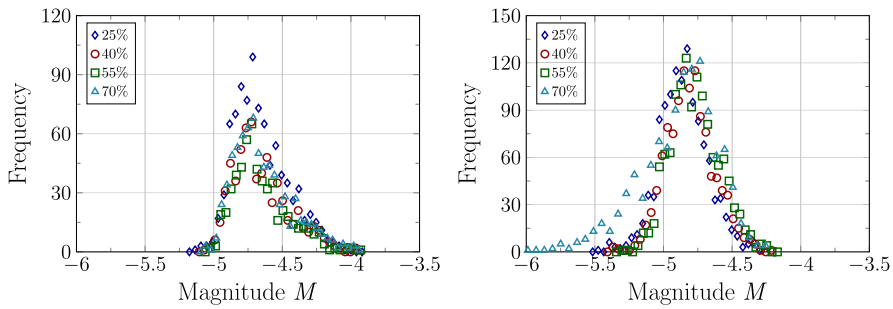

Fig. 41 The relationship between AE magnitude and frequency in samples with different quartz content at room temperature and after thermal treatment at 600°C

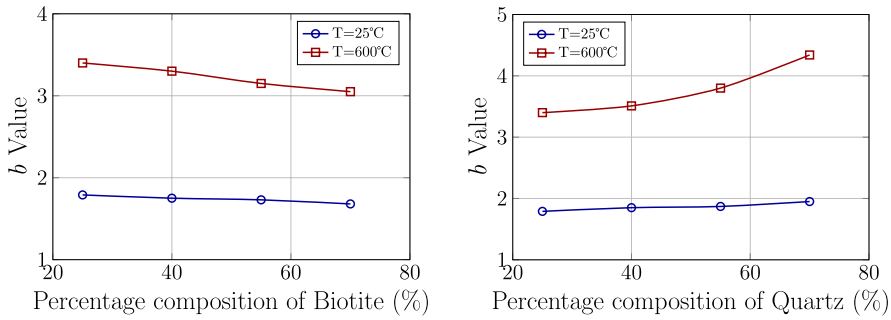

(a) Effect of biotite content on b value (b) Effect of quartz content on b value

Fig. 42 Effect of biotite and quartz content on b value

conditions, the lower thermal expansion coefficient of biotite plays a key role in the overall thermal stability of the rock. As the content of biotite increases, the rock's thermal stability improves, reducing the formation of thermally induced cracks, and thus the b value decreases with increasing biotite content. In contrast, quartz has a higher thermal expansion coefficient, and at the same heat treatment temperature, the number of thermally induced cracks in the sample increases with the increase in quartz content. Under external loading, the sample is more likely to fail, with the majority of the AE events being small magnitude events. Therefore, the b value increases as the quartz content rises.

7 Discussions and limitation

Figure 43 summarizes the peak strength loss rates at 600°C from this study and the research by Hu et al. (2023). Both studies utilized the method of Liu et al. (2018) for calculating the heterogeneity index. Despite differences in grain shape, mineral composition, and grain size distribution among minerals in the models, the peak strength loss rate increases with the heterogeneity index in both studies. However, since Hu et al.'s research did not account for the effect of mineral physicochemical reactions on rock thermal damage, the fitted curve in Fig. 43a indicates that the strength loss rate for samples with different heterogeneity index in their study is lower than that found in this study. This suggests that their research may have underestimated the thermal damage caused by temperature on rocks.

Figure 43b summarizes the strength loss rates at 600°C for samples with different grain sizes. Kang et al. (2021) and Shao et al. (2014) experimentally investigated the physical and mechanical changes in three different grain-sized granites after thermal treatment, analyzing the distribution of grain sizes, thermally induced cracks, and fracture evolution under uniaxial compression test. The x-axis labels 1, 2, and 3 in Fig. 43b correspond to fine-grained, medium-grained, and coarse-grained granites of their studies,

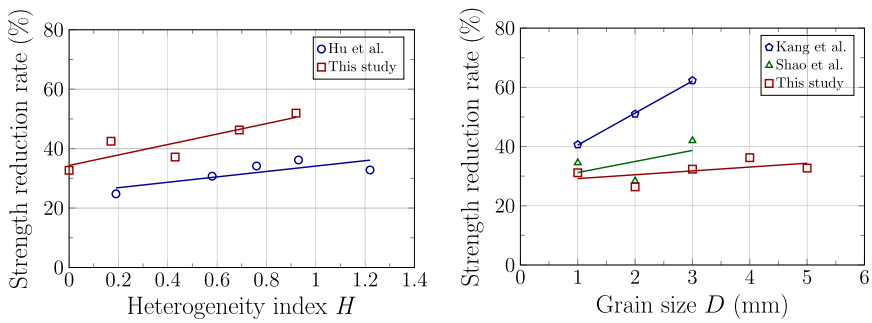

(a) The relationship between grain size heterogeneity and strength reduction rate(b) The relationship between grain size and strength reduction rate

Fig. 43 Strength loss rate of samples with different grain size heterogeneity index and grain sizes after 600°C treatment

respectively. Although the conclusions from numerical simulations and experiments regarding the relationship between grain size and peak strength at room temperature differ, the strength loss rates at high temperatures follow a consistent pattern, showing a positive correlation between strength loss rate and grain size.

In this study, the sample with a grain size heterogeneity index of 0 exhibited a strength loss rate of 32.72% at 600°C, the lowest among the models with different heterogeneity index. The sample with a grain size of 3.38 mm, corresponding to a heterogeneity index of 0, showed the highest strength loss rate at 600°C among the samples with different grain sizes. Combining Fig. 43a and b, it is evident that grain size heterogeneity is the primary factor influencing the mechanical properties of crystalline rocks, whether at room temperature or high temperature. At room temperature, the more uneven the grain size distribution in the sample, the lower the peak strength. When exposed to high temperatures, the strength loss rate also increases. Only when the grain size distribution is relatively uniform does the grain size affect the peak strength.

In laboratory experiments, the study of mineral content's effect on rock mechanical properties is often susceptible to interference from extraneous factors, making it challenging to control as a variable. As shown in Fig. 17, the peak strength of samples varies considerably with different mineral contents. Compared to the relationships between grain size heterogeneity index, grain size, and peak strength, the correlation between mineral composition and peak strength is less significant. After accounting for the effects of mineral shape and grain size, Fig. 17 indicates that at room temperature, the peak strength of the samples decreases slightly with increasing quartz content, but the reduction is minimal. We also analyzed the relationship between the content of K-feldspar and plagioclase and peak strength. However, due to space limitations, this was not discussed in detail. The results show that, at room temperature, the relationship between the mineral composition of K-feldspar and plagioclase and peak strength is similarly weak.

At a thermal treatment temperature of 600°C, the reduction in peak strength is more pronounced compared to room temperature. A close examination of the fitted curve at 600°C in Fig. 17 reveals that the significant decrease in the curve's slope is primarily due to the three data points corresponding to quartz content below 20%, which are notably higher in peak strength than those with quartz content above 20%. These three values correspond to the peak strengths of models M2, M3, and M9, as shown in Table 3. K-feldspar and plagioclase, considered relatively "neutral" minerals in the samples, have moderate thermal expansion coefficients. These minerals can somewhat mitigate stress concentration caused by the expansion differences between quartz and other minerals, thereby reducing the formation and propagation of microcracks. This supportive role of K-feldspar and plagioclase becomes more significant at higher temperatures, making their content positively correlated with peak strength in high-temperature conditions.

Thus, it can be concluded that at room temperature, when the grain size distribution in the sample is relatively uniform, the influence of mineral content on the peak strength is less than in samples with uneven grain size distribution. Under high-temperature conditions, increasing the content of relatively "neutral" minerals (with moderate thermal expansion coefficients) in the sample can mitigate the effects of temperature on the thermal damage of crystalline rocks.

In summary, whether under room temperature or high-temperature conditions, the non-uniform distribution of grain size has the most significant effect on peak strength. It is the primary factor affecting the mechanical properties of crystalline rocks. Given the inconsistencies between numerical simulations and experimental results regarding the influence of grain size on the mechanical properties of crystalline rocks at room temperature, we will not explore this further. At the same temperature, when the grain size distribution in the sample is relatively uniform, samples with smaller grain sizes exhibit higher mechanical stability than those with larger grain sizes, making this a secondary factor. Regardless of temperature, the effect of mineral composition on the sample's mechanical properties is less significant than that of grain size heterogeneity and grain size itself. Hemmati et al. (2020) also demonstrated that grain size substantially influences rock strength more than mineral content. For example, in the context of selecting a site for a nuclear waste repository, the above analysis suggests that granite with a uniform grain size distribution, smaller grain sizes, and a higher content of relatively "neutral" minerals (with moderate thermal

expansion coefficients) should be preferred to prevent the leakage of radioactive nuclear waste effectively.

Indeed, this study has certain limitations. As discussed in Sect. 4.1.2, the distribution of minerals with different thermal expansion coefficients and hardness in the numerical model could still significantly affect the results under high-temperature conditions. For instance, if a specific mineral with the highest or lowest thermal expansion coefficient is predominantly present in a localized area or minerals with the greatest difference in thermal expansion coefficients are in close contact, these factors could lead to varying outcomes. Additionally, when analyzing grain size and mineral content, this study controlled the grain shapes to be regular hexagons. However, minerals in natural rocks exhibit complex geometries, and irregularly shaped minerals may have more edges and corners, which can act as stress concentration points under thermal stress, leading to increased local stress. Přikryl (2001) have shown that the preferred orientation of mineral shapes influences the anisotropy of rock strength. As the degree of preferred mineral alignment increases, strength anisotropy becomes more pronounced, highlighting the complexity of failure mechanisms in crystalline rocks. Future research should focus on these factors. Nonetheless, this study offers valuable insights into the thermal damage mechanisms of crystalline rocks and the effects of geometric and property heterogeneity on their mechanical properties and failure mechanisms.

8 Conclusion

This study employed the DEM to investigate the thermal damage mechanisms in crystalline rocks, focusing on analyzing the effects of grain size heterogeneity, grain size, and mineral composition on the thermomechanical response and failure mechanisms. Additionally, based on the moment tensor inversion theory, a method for simulating AE during rock failure at the microscale was established. The analysis of AE events provided insights into the effect of rock heterogeneity on failure mechanisms and micro-seismic behavior. The main conclusions are as follows:

(1) Peak strength decreases with increasing grain size heterogeneity, while the heterogeneity index has a smaller effect on elastic modulus. Peak strength increases with grain size, but at higher thermal treatment temperatures, elastic modulus decreases with increasing grain size. Quartz content negatively correlates with peak strength, with the effect becoming more pronounced at higher temperatures. Between 25~450°C, a positive correlation exists between quartz content and the elastic modulus; however, this relationship reverses to a negative correlation when the thermal treatment temperature reaches 600°C.
(2) The number of thermally induced cracks and the maximum contact force both increase with grain size heterogeneity and thermal treatment temperature. In samples with uniform grain size distribution, stress is more evenly distributed, resulting in greater contact force. Thermal stress in heated samples is influenced by grain size, mineral shape, and arrangement. Irregular mineral particles, with more corners and edges, are more prone to stress concentration under thermal conditions.
(3) As grain size increases, intergranular cracks decrease and intragranular cracks increase. The total number of thermally induced cracks decreases with larger grain sizes. Due to their greater volume and relatively fewer boundaries, larger grains are more prone to significant stress concentration during phase changes and melting, leading to higher contact forces in large-grain models. As quartz content increases, thermally induced cracks rise, and contact force increases with minerals having higher thermal expansion coefficients.
(4) As the grain size heterogeneity index increases, the b value increases. The combined effect of high temperatures and grain size heterogeneity results in a more pronounced increase in b values in models with higher grain size heterogeneity index. Conversely, the b value decreases with increasing grain size. Smaller grains complicate crack paths, leading to more frequent reflections, twists, or branches at grain boundaries. While low in energy, these activities occur at a high frequency, thus contributing to a higher b value. For any sample, the distribution range of AE magnitudes is generally lower after thermal treatment compared to room temperature conditions.
(5) Under both room and high temperature conditions, grain size heterogeneity most significantly

affects sample stability, making it the primary factor influencing the mechanical properties of crystalline rocks. At the same temperature, samples with uniform grain size distribution show higher thermal stability with smaller grains, making grain size the secondary factor influencing the mechanical properties of crystalline rocks. Regardless of temperature, mineral composition has less impact on mechanical performance than grain size heterogeneity and grain size.

Acknowledgements Thanks to the Xi'an Jiaotong University Innovation Talents Program for sponsoring this research.

Author contributions YK.D: wrote the manuscript, Z.Y: provided research ideas for the article, ST.Y: provided research ideas and grant support for the article, XY.L: created figures and tables, JL.S: provided software and English writing guidance.

Funding The study was gratefully funded by the Science and Technology Program of Xuzhou (Grant No. KC23428), China.

Declarations

Conflict of interest The authors declare that they have no conflict of interest.

References

Ramzy AK, Abdelaziz A, Fekadu HB, Qi Z, Giovanni G (2024) Evaluation of damage stress thresholds and mechanical properties of granite: new insights from digital image correlation and gb-fdem. Rock Mech Rock Eng 57(7):4679–4706

Åkesson U (2008) Characterization of micro cracks using core disking. Technical report, SKB Report P-08-103. Stockholm: Swedish Nuclear Fuel and Waste Manage Co

Asemi F, Lakirouhani A, Nicksiar M, Zohdi A (2024) A new rock brittleness index based on crack initiation and crack damage stress thresholds. Int J Geomech 24(5):04024074

Bass Jay D et al (1995) Elasticity of minerals, glasses, and melts. Min Phys Crystallogr: Handbook Phys Constants 2:45–63

Blair SC, Cook NGW (1998) Analysis of compressive fracture in rock using statistical techniques: part ii. Effect of microscale heterogeneity on macroscopic deformation. Int J Rock Mech Min Sci 35(7):849–861

Blair SC, Cook NGW (1998) Analysis of compressive fracture in rock using statistical techniques: part i. A nonlinear rule-based model. Int J Rock Mech Min Sci 35(7):837–848

Chen Y, Yin T, Li X, Li Q, Yang Z, Li M, You W (2021) Experimental investigation on dynamic mechanical behavior and fracture evolution of fissure-filled red sandstone after thermal treatment. Eng Geol 295:106433

Cheng T, Wang L, Xiao Y, He M, Wang T, Peng M, Li H (2023) Correlational fractal characteristics and damage progression of granite with different grain sizes based on acoustic emission monitoring. Eng Geol 327:107358

Cowie S, Walton G (2018) The effect of mineralogical parameters on the mechanical properties of granitic rocks. Eng Geol 240:204–225

Dang Y, Yang Z, Liu X (2023) Three-dimensional numerical study on failure mechanism of granite after thermal treatment based on moment tensor inversion. Comput Geotech 155:105185

Dang Y, Yang Z, Liu X, Chunting L (2023) Numerical study on failure mechanism and acoustic emission characteristics of granite after thermal treatment. Comput Particle Mech 10(5):1245–1266

Dang Y, Yang Z, Zhu H(2023) Study on failure mechanism of tight sandstone based on moment tensor inversion. *Heliyon*, 9(8)

Dang Y, Yang Z, Liu X(2024) Revealing the influence of grain size on failure mechanisms and acoustic emission characteristics in thermally treated crystalline rock: insights from moment tensor inversion. Rock Mechanics and Rock Engineering, pages 1–33

Dang Y, Yang Z, Liu X, Guo J (2024) Crack propagation mechanism in bedded rock with parallel flaws: insights from moment tensor inversion. Theoret Appl Fract Mech 129:104180

Dang Y, Yang Z, Yang S, Shang J (2024c) Thermal damage in crystalline rocks: The role of heterogeneity in mechanical performance and fracture mechanisms. In: ARMA US Rock Mechanics/Geomechanics Symposium, pages ARMA–2024. ARMA

Kun D, Sun Yu, Zhou J, Khandelwal M, Gong F (2022) Mineral composition and grain size effects on the fracture and acoustic emission (AE) characteristics of rocks under compressive and tensile stress. Rock Mech Rock Eng 55(10):6445–6474

Eberhardt E, Stead D, Stimpson B (1999) Quantifying progressive pre-peak brittle fracture damage in rock

during uniaxial compression. Int J Rock Mech Min Sci 36(3):361–380
Erik E, Stimpson B, Doug S (1999) Effects of grain size on the initiation and propagation thresholds of stress-induced brittle fractures. Rock Mech Rock Eng 32:81–99
Gui YL, Zhao ZY, Jian J, Wang XM, Zhou KP, Ma SQ (2016) The grain effect of intact rock modelling using discrete element method with voronoi grains. Géotechnique Letters 6(2):136–143
Guo P, Zhang P, Bu M, Wang Z, Zheng X, and He M (2023) Microcracking behavior and damage mechanism of granite subjected to high temperature based on ct-gbm numerical simulation. Computers and Geotechnics 159:105385
Gutenberg B (2013) Seismicity of the earth and associated phenomena. Read Books Ltd
Hamediazad F, Bahrani N (2024) Evaluation of the rock mass strength for hard rock pillar design using bonded block models. Rock Mech Rock Eng 57(5):3659–3680
Han Z, Zhang L, Azzam R, Zhou J, Wang S (2021) A statistical index indicating the degree and mechanical effects of grain size heterogeneity in rocks. Eng Geol 293:106292
Farhana HN, Jimoh Onimisi A, Abdulazeez SS, Zabidi H (2019) The effect of mineralogical composition on strength and drillability of granitic rocks in Hulu Langat, Selangor Malaysia. Geotech Geol Eng 37:5499–5505
He C, Mishra B, Shi Q, Zhao Y, Lin D, Wang X (2023) Correlations between mineral composition and mechanical properties of granite using digital image processing and discrete element method. Int J Min Sci Technol 33(8):949–962
He C, Mishra B, Yuan W, Wang X, Shi Q (2024) Investigation of the dynamic behavior and fracturing mechanism of granite. Fuel 360:130579
Hemmati A, Ghafoori M, Moomivand H, Lashkaripour GR (2020) The effect of mineralogy and textural characteristics on the strength of crystalline igneous rocks using image-based textural quantification. Eng Geol 266:105467
Hofmann H, Babadagli T, Yoon JS, Zang A, Zimmermann G (2015) A grain based modeling study of mineralogical factors affecting strength, elastic behavior and micro fracture development during compression tests in granites. Eng Fract Mech 147:261–275
Xunjian H, Haibo H, Xie N, Huang Y, Guo P, Gong X (2023) The effect of grain size heterogeneity on mechanical and microcracking behavior of pre-heated lac du bonnet granite using a grain-based model. Rock Mech Rock Eng 56(8):5923–5954
Kang F, Li Y et al (2021) Grain size heterogeneity controls strengthening to weakening of granite over high-temperature treatment. Int J Rock Mech Min Sci 145:104848
Kelly DD, Peck DC, James RS (1994) Petrography of Granitic Samples from the 420 m Level of the Underground Research Laboratory. Manitoba, report, Laurentian Univ., Sudbury, Ont., Canada, Pinawa
Kong L, Ranjith PG, Li BQ (2021) Fluid-driven micro-cracking behaviour of crystalline rock using a coupled hydro-grain-based discrete element method. Int J Rock Mech Min Sci 144:104766
Kong L, Shang J, Gamage RP, Li BQ, Song Y, Cai W, Ling F (2024) Grain-based dem modelling of mechanical and coupled hydro-mechanical behaviour of crystalline rocks. Engineering Geology, page 107649
Lakirouhani A, Asemi F, Zohdi A, Medzvieckas J, Kliukas R (2020) Physical parameters, tensile and compressive strength of dolomite rock samples: influence of grain size. J Civ Eng Manag 10:789–799
Lakirouhani A, Bakhshi M, Zohdi A, Medzvieckas J, Gadeikis S (2022) Physical and mechanical properties of sandstones from Southern Zanjan, North-western Iran. Baltica 35(1):23–36
Lan H, Martin CD, Hu B (2010) Effect of heterogeneity of brittle rock on micromechanical extensile behavior during compression loading. J Geophys Res: Solid Earth, 115(B1)
Liu G, Cai M, Huang M (2018) Mechanical properties of brittle rock governed by micro-geometric heterogeneity. Comput Geotech 104:358–372
Ma Q, Liu X, Wang E, Liu C, Jia W (2024) Optimizing 3d granular modeling with integrated 3dec and neper techniques for granite mechanics simulation. Comput Geotech 173:106578
Martin CD (1993) The strength of massive Lac du Bonnet granite around underground openings. PhD thesis, University of Manitoba
Meng Z, Pan J (2007) Correlation between petrographic characteristics and failure duration in clastic rocks. Eng Geol 89(3–4):258–265
Nasseri M, Schubnel A, Young RP (2007) Coupled evolutions of fracture toughness and elastic wave velocities at high crack density in thermally treated westerly granite. Int J Rock Mech Min Sci 44(4):601–616
Nicksiar M, Martin CD (2014) Factors affecting crack initiation in low porosity crystalline rocks. Rock Mech Rock Eng 47:1165–1181
Peng J, Wong LNY, Teh CI (2017) Effects of grain size-to-particle size ratio on micro-cracking behavior using a bonded-particle grain-based model. Int J Rock Mech Min Sci 100:207–217
Peng J, Wong LNY, Teh CI (2017) Influence of grain size heterogeneity on strength and microcracking behavior of crystalline rocks. J Geophys Res: Solid Earth 122(2):1054–1073
Peng J, Wong LNY, Teh CI (2021) Influence of grain size on strength of polymineralic crystalline rock: new insights from dem grain-based modeling. J Rock Mech Geotech Eng 13(4):755–766
Potyondy DO (2010) A grain-based model for rock: approaching the true microstructure. Proceedings of rock mechanics in the Nordic Countries, pages 9–12
Potyondy DO, Cundall PA (2004) A bonded-particle model for rock. Int J Rock Mech Min Sci 41(8):1329–1364
Přikryl R (2001) Some microstructural aspects of strength variation in rocks. Int J Rock Mech Min Sci 38(5):671–682
Sajid M, Coggan J, Arif M, Andersen J, Rollinson G (2016) Petrographic features as an effective indicator for the variation in strength of granites. Eng Geol 202:44–54
Shang J (2020) Rupture of veined granite in polyaxial compression: insights from three-dimensional discrete element method modeling. J Geophys Res: Solid Earth 125(2):e2019JB019052

Shao S, Wasantha PLP, Ranjith PG, Chen BK (2014) Effect of cooling rate on the mechanical behavior of heated strathbogie granite with different grain sizes. Int J Rock Mech Min Sci 70:381–387

Shao S, Ranjith PG, Wasantha PL, Chen BK (2015) Experimental and numerical studies on the mechanical behaviour of Australian Strathbogie granite at high temperatures: an application to geothermal energy. Geothermics 54:96–108

Shi C, Yang W, Yang J, Chen X (2019) Calibration of micro-scaled mechanical parameters of granite based on a bonded-particle model with 2d particle flow code. Granular Matter 21(2):38

Shi C, Zhang Y, Zhang Y, Chen X, Yang J (2023) Microdamage study of granite under thermomechanical coupling based on the particle flow code. Front Struct Civ Eng 17(9):1413–1427

Sousa LMO (2013) The influence of the characteristics of quartz and mineral deterioration on the strength of granitic dimensional stones. Environmental earth sciences 69:1333–1346

Sun W, Shunchuan W, Xueliang X (2021) Mechanical behaviour of lac du bonnet granite after high-temperature treatment using bonded-particle model and moment tensor. Comput Geotech 135:104132

Tang L, Zihan L, Zheng J, Zheng J, Jin L, Yongtang Yu, Jia H, Sun Q, Di W, Li G (2023) Mechanism of strength degradation of frozen soil-rock mixture under temperature rise-induced particle ice film ablation. Permafrost Periglac Process 34(4):530–546

Tang L, Sun S, Zheng J, Qiu P, Guo T (2023) Thermal conductivity changing mechanism of frozen soil-rock mixture and a prediction model. Int J Heat Mass Transf 216:124529

Tian W-L, Yang S-Q, Huang Y-H, Bo H (2020) Mechanical behavior of granite with different grain sizes after high-temperature treatment by particle flow simulation. Rock Mech Rock Eng 53:1791–1807

Wang F, Konietzky H (2019) Thermo-mechanical properties of granite at elevated temperatures and numerical simulation of thermal cracking. Rock Mech Rock Eng 52:3737–3755

Wang F, Konietzky H, Herbst M (2019) Influence of heterogeneity on thermo-mechanical behaviour of rocks. Comput Geotech 116:103184

Wang F, Konietzky H, Frühwirt T, Dai Y (2020) Laboratory testing and numerical simulation of properties and thermal-induced cracking of eibenstock granite at elevated temperatures. Acta Geotech 15:2259–2275

Wang F, Konietzky H, Herbst M, Chen W (2022) Mechanical responses of grain-based models considering different crystallographic spatial distributions to simulate heterogeneous rocks under loading. Int J Rock Mech Min Sci 151:105036

Wang F, Meng D, Ke H, Xun D, Pang R, Zou Y, Dang W, He B (2024) Thermo-mechanical coupling characteristics of granite under triaxial pressures and ultrahigh heating rates. Comput Geotech 167:106098

Wang X, Sun W, He C, Yuan W, Sarfarazi V, Wang H (2024b) Fracturing behaviors of flawed granite induced by dynamic loadings: A study based on dip and pfc. Deep Underground Science and Engineering

Wong Louis N, Peng J, Teh CI (2018) Numerical investigation of mineralogical composition effect on strength and micro-cracking behavior of crystalline rocks. J Nat Gas Sci Eng 53:191–203

Zhijun W, Li M, Weng L (2020) Thermal-stress-aperture coupled model for analyzing the thermal failure of fractured rock mass. Int J Geomech 20(10):04020176

Yan D, Zhao L, Wang Y, Zhang Y, Cai Z, Song X, Zhang F, Geng J (2023) Heterogeneity indexes of unconventional reservoir shales: quantitatively characterizing mechanical properties and failure behaviors. Int J Rock Mech Min Sci 171:105577

Yang Z, Dang Y, Yang S, Liu X (2024) Analysis of mechanical properties and failure modes in thermally treated granite with structural defects. In: ARMA US Rock Mechanics/Geomechanics Symposium, pages ARMA–2024. ARMA

Yılmaz NG, Mete Goktan R, Kibici Y (2011) Relations between some quantitative petrographic characteristics and mechanical strength properties of granitic building stones. Int J Rock Mech Min Sci 48(3):506–513

Zhang S, Qiu S, Jiang Q, Wang B, Xunjian H, Zhang H (2023) Numerical study of unstable failure behavior in heterogeneous rock pillar. Eng Fract Mech 290:109529

Zhang X-P, Wong LNY (2014) Choosing a proper loading rate for bonded-particle model of intact rock. Int J Fract 189:163–179

Zhao H, Zhang L, Zhonghuai W, Liu A (2022) Fracture mechanisms of intact rock-like materials under compression. Comput Geotech 148:104845

Zhao Z, Haoran X, Wang J, Zhao X, Cai M, Yang Q (2020) Auxetic behavior of beishan granite after thermal treatment: a microcracking perspective. Eng Fract Mech 231:107017

Zhou Yu, Lv W, Li B, Liang Q (2024) Impact of soft minerals on crack propagation in crystalline rocks under uniaxial compression: a grain-based numerical investigation. Int J Numer Anal Meth Geomech 48(8):2020–2042